Supplementary Material for:

Title: Culture-independent discovery of the malacidins as calcium-dependent antibiotics with activity against multidrug-resistant Gram-positive pathogens.

Authors: Bradley M. Hover[1], Seong-Hwan Kim[1], Micah Katz[1], Zachary Charlop-Powers[1], Jeremy G. Owen[1], Melinda A. Ternei[1], Jeffrey Maniko[1], Andreia Estrela[1], Henrik Molina[2], Steven Park,[3] David S. Perlin,[3] and Sean F. Brady[1]*

Corresponding Author: Sean F. Brady
Contact: Laboratory of Genetically Encoded Small Molecules
The Rockefeller University
1230 York Avenue
New York, NY 10065
Phone: 212-327-8280
Fax: 212-327-8281
Email: sbrady@rockefeller.edu

Table of Contents:

Supplemental Discussion

Structure determination of malacidins A and B.

NMR and MS analysis: Malacidin A was isolated as a white powder at a yield of 6 mg L^{-1} of *S. albus* DFD0097-644:735:388 culture. The molecular formula was obtained as $C_{56}H_{88}N_{12}O_{20}$ by HRESIMS (experimental $[M+H]^+$ = 1249.6295, calc'd $[M+H]^+$ for $C_{56}H_{89}N_{12}O_{20}$ = 1249.6316), and confirmed by ^1H and ^{13}C and edited HSQC NMR spectra. Through COSY, TOCSY, and HMBC NMR analysis, the partial structures of 10 amino acids and an unsaturated fatty acid were developed. The ten amino acid groups were an aspartic acid, two 3-methyl aspartic acids (MeAsp), a 3-hydroxyl aspartic acid (HyAsp), a 2,3-diamino 3-methyl propanoic acid (MeDap), a 4-methyl proline (MePro), two valines (Val), a lysine (Lys), and a glycine (Gly). Based on ^1H NMR and edited HSQC NMR spectra, 4 deshielded olefinic protons, 10 amide alpha protons from δ_H 4.85 to δ_H 3.98 coupled with δ_C 60.3 to δ_C 42.6, an oxymethine proton δ_H 4.58, 7 methyl methine protons, 9 methylene protons, and 10 methyl protons were revealed. The ^{13}C NMR spectrum indicated 15 carbonyl carbons (δ_C 177.4~169.5), 4 olefinic carbons (δ_C 143.3~121.6), and 10 methyl carbons. The HMBC correlations from δ_H 3.13 and 1.23 to δ_C 177.4 and from δ_H 3.06 and 1.21 to δ_C 177.4, indicating the connections of carboxyl acids, established two methyl aspartic acids. The hydroxyl aspartic acid was developed by the HMBC correlation between δ_H 4.58 (connected with δ_C 70.5) and δ_C 174.5. The β methine carbon of diamino methyl propanoic acid was developed by the empirical ^1H-^{13}C chemical shift of δ_H 4.27-δ_C 47.8 indicating a nearby nitrogen atom. The 4-methyl proline amino acid was supported by HMBC correlations between δ_H 3.79, 3.43, 2.48, 1.96, and 1.86 and δ_C 16.8. The valine and lysine amino acids were also established by HMBC correlations. The COSY correlations of olefinic protons between δ_H 7.64, 6.24, 6.18, and 6.03 indicated a diene functional group and the HMBC correlations between δ_H 6.18 and δ_C 169.5 supported an α,β-unsaturated carbonyl functional group. Through further COSY and HMBC analysis, methyl nonadienoic acid was fully determined. The geometries of methyl nonadienoic acid were determine by measuring coupling constants, δ_H 6.18 (d, *J*=15Hz), δ_H 7.64 (dd, *J*=15, 11Hz), δ_H 6.24 (dd, *J*=11, 11Hz), and δ_H 6.03 (ddd, *J*=11, 7.5, 7.5Hz) in sequence.

Based on the structures of 10 partial amino acids and a fatty acid, the five connected partial structures were developed by HMBC correlations between the α proton of amino acids and two carbonyl carbons of neighboring two amino acids. The HMBC correlations from δ_H 6.18 and 4.85 to δ_C 169.5 indicated the connection between methyl nonadienoic acid and MeAsp. The HMBC correlations from δ_H 4.39, 1.97, 1.86, and 4.27 to δ_C 173.8 indicated a MeDap-MePro residue. The MeAsp-Val residue was developed by HMBC correlations between δ_H 4.70, 4.03 and δ_C 171.4. The Lys-HyAsp-Asp-Gly residue was also constructed by HMBC correlations. To overcome the missing HMBC correlation among 5 residues and confirm the planar structure of malacidin A, the propionate derivative of malacidin A was made by reaction with propionic anhydride. The existence of a lysine was confirmed by more than 56 Da of a primary amine. The structure of propionic malacidin A was deduced by HRESI-MS/MS fragmentation experiments. Through MS/MS fragmentation analysis, the major ion value 433.1200 indicated the sequence connection of HyAsp-Asp-Gly-MeAsp including a Lys-HyAsp-Asp-Gly block, which was developed by HMBC. The major ion value 774.4767 supported the connection of two blocks between Lys-HyAsp-Asp-Gly and MeAsp-Val. The major fragment ion 280.1542 was confirmed as a Methylnonadienoic acid-MeAsp block. The major fragment ion 1026.5110 possessed the total value of 4 building blocks. Through fragmentation analysis, 774.4767, 590.3550, and 491.2865 ions were deduced to be a sequence from methylnonadienoic acid to propionate lysine.

Malacidin B was isolated as white powder at a yield of 2.5 mg L^{-1} of *S. albus* DFD0097-644:735:388 culture. Its molecular formula was determined to be $C_{57}H_{90}N_{12}O_{20}$ by HRESIMS (found *m*/*z* 1263.6484, calcd for $C_{57}H_{91}N_{12}O_{20}$, 1263.6473). The 14 Dalton difference of molecular formula between 1 and 2 suggested that malacidin B was an analogue of A. The COSY, TOCSY, and HMBC analysis of malacidin B illustrated an additionally CH_2 bond on the unsaturated fatty acid moiety. The triplet (δ_H 0.86) and doublet (δ_H 0.89) methyl proton signals suggests methyl decadienoic acid as the N-terminal fatty acid of malacidin B. Through HRESI-MS/MS fragmentation experiments, malacidins A and B were confirmed to possess the same cyclic core peptide, strongly supporting the proposal that malacidin B is only different on the fatty acid side chain compared to malacidin A.

Bioinformatic analysis: Support for the general structure of the malacidins was provided by a detailed bioinformatics analysis of the malacidin BGC (GenBank Accession KY654519). Four genes of the malacidin BGC are predicted to encode for nonribosomal peptide synthetases (MlcA and MlcK-M). Within this collection

of NRPSs, there are a total of 10 adenylation domains, corresponding to the production of a 10-amino acid peptide (**Supplemental Figures S23-S25**). Genes predicted to encode the biosynthesis of three of the four non-proteinogenic amino acids present in the malacidins were easily identified in the malacidin BGC (**Supplemental Data Table S3, Fig. S23-S25)**. Only the origin of the 3-hydroxyl aspartic acid is not immediately obvious from our gene prediction analyses. The 3-methyl aspartic acids are likely produced by MlcE and MlcF, which show high sequence similarity to proteins GlmA and GlmB from the cobalamin-dependent glutamate mutase complex used to produce the same amino acid in friulimicin biosynthesis.[1] MlcP-R are related to GriH, GriF/nosE and GriE, which are responsible for 4-methyl proline production in griselimycin and nostopeptolide biosyntheses.[2, 3] Similarly, MlcT and MlcS share high sequence similarity to DabB and a fused DabC-A protein from *Actinoplanes friuliensis*, which are essential for 2,3-diamino 3-methyl propanoic acid.[4] Additionally, MlcG-J are predicted to be involved in the synthesis (MlcG), desaturation (MlcHI), and incorporation (MlcJ) of the *N*-terminal fatty acid component to malacidin A.[4, 5]

Stereochemical analysis: Epimerization domains located at the ends of the MlcK and MlcL NRPSs are predicted to change the stereochemistry of the Val at position 3 and the MeAsp at position 8 from an $_{L}$-configuration to a $_{D}$-configuration. To empirically support these and the rest of the stereochemical predictions, we used Marfey's reagent to analyze the amino acids in both malacidin A and B. Initially, malacidin A and B were individually hydrolyzed under acidic conditions. The hydrolyzed amino acids were derivatized with Marfey's reagents ($_{L,D}$-FDAA) and the resulting Marfey's derivatives were analyzed by LC/MS to determine the absolute configuration for each amino acid (**Supplemental Data Table S3, Fig. S21-S22**). Based on the elution order of diasteromer standards tested in-house as well as elution order data from the literature, the absolute configuration of $_{L}$-Lys, $_{L}$-HyAsp and $_{L}$-Asp, were readily determined.[6, 7] As predicted bioinformatically we observed both $_{D}$-Val and $_{L}$-Val. These configurations are identical for both malacidin A and B and match the bioinformatic predictions in all cases. The relative configuration of C-2 and C-4 in $_{L}$-MePro was determined both by Marfey's analysis of the commercial standard, (2*S*,4*R*)-4-methylpyrrolidine-2-carboxylic acid, and through a ROESY NMR experiment (**Supplemental Figures S19-S20**). Due a lack of readily available commercial standards for $_{LD}$-MeDap and $_{LD}$-MeAsp, not all of the stereochemistry configurations in malacidin could be resolved by Marfey's analysis or NMR. We were however able to predict through bioinformatics analysis the likely stereochemistry of the α-carbons for residues 1, 2, and 8 to be $_{L}$-MeAsp, $_{L}$-MeDap, and $_{D}$-MeAsp, respectively (**Supplemental Figures S23-S25**). These were determined through a detailed comparison of the chemical and biosynthetic similarities between the MeDap and MeAsp residues in malacidin to that of residues found in other evolutionarily related $_{LD}$-MeDap, $_{LD}$-Dap, or $_{LD}$-MeAsp containing molecules.[4, 8-10] For example, the malacidin gene cluster encodes for homologs to the DabA, DabB, DabC enzymes that transfer an amine from $_{L}$-Orn to $_{L}$-Thr to yield a stereospecific $_{L}$-*threo*-MeDap in fruilimicin biosynthesis.[4] Sharing a similar domain structure as fruilimicin at the position, it is likely that malacidin incorporates an identical $_{L}$-MeDap. In a similar scope, the malacidin gene cluster shares related enzymes to fruilimicin for the biosynthesis of 3-methylaspartic acids. These cobalamin-dependent glutamate mutase enzymes, GlmA and GlmB, produce $_{L}$-*threo*-3-MeAsp from $_{L}$-Glu in friulimicin biosynthesis. While malacidin gene cluster incorporates two 3-methylaspartic acids (position 1 & 8), the second is encoded by a NRPS module in the MlcL synthetase that contains an epimerization domain that is responsible for changing the stereochemistry to $_{D}$-MeAsp.

Table S1. Malacidin biosynthetic gene cluster analysis
39 predicted ORFs constituted the malacidin BGC (ORFS 1-39) -- 26 of which (mlcA-Z) have similarities to genes found in characterized NRPS BGCs.[4, 5, 8, 10, 11]

ORF	Gene Size (bp)	Gene Name	Proposed Function	Protein [Organism], NCBI Gene Bank Accession Number Corresponding to Gene with Sequence Similarity	E-value	Protein ID%
1	459	orf1	Unknown	hypothetical protein [Amycolatopsis taiwanensis], WP_027945115	1.0E-62	89%
2	774	orf2	Unknown	Nucleoside-diphosphate-sugar epimerase [Saccharopolyspora shandongensis], SDW57388	3.0E-146	87%
3	927	orf3	Unknown	RNA polymerase, sigma subunit, ECF family [Saccharopolyspora shandongensis], SDW57388	9.0E-177	90%
4	3132	**mlcA**	Peptide Synthesis	non-ribosomal peptide synthetase [Actinoplanes friuliensis], WP_023362349	0	54%
5	897	**mlcB**	Possible Regulator	GHMP kinase [Actinoplanes friuliensis], WP_023362350	2.0E-114	65%
6	939	**mlcC**	Regulation	SyrP [Streptomyces ambofaciens], WP_053138577	2.0E-157	72%
7	816	**mlcD**	Transport/Resistance	ABC transporter permease [Streptomyces ambofaciens], WP_063484561	1.0E-76	56%
8	1218	**mlcE**	3-Methylaspartic Acid Biosynthesis	methylaspartate mutase, E-chain [Streptomyces sp. NRRL S-350], WP_030245251	2.0E-163	63%
9	474	**mlcF**	3-Methylaspartic Acid Biosynthesis	methylaspartate mutase, S-chain [Streptomyces sp. NRRL S-350], WP_030245253	4.0E-41	57%
10	1764	**mlcG**	Acyl-CoA/AMP Synthesis	acyl-CoA synthase [Actinoplanes friuliensis], WP_023362355	7.0E-180	52%
11	1434	**mlcH**	Desaturation of Acyl Chain	acyl-CoA dehydrogenase [Streptomyces sp. MBT76], WP_058042025	7.0E-151	54%
12	1596	**mlcI**	Desaturation of Acyl Chain	acyl-CoA dehydrogenase [Streptomyces ambofaciens], WP_064384562	0	55%
13	270	**mlcJ**	Attachment of the Acyl Chain	acyl carrier protein [Streptomyces sp. DvalAA-43], SCD55195	1.0E-19	54%
14	9195	**mlcK**	Peptide Synthesis	non-ribosomal peptide synthetase B [Actinoplanes friuliensis], CAJ18237	0	50%
15	16887	**mlcL**	Peptide Synthesis	non-ribosomal peptide synthetase C [Actinoplanes friuliensis], WP_023362360	0	52%
16	6843	**mlcM**	Peptide Synthesis	non-ribosomal peptide synthetase D [Actinoplanes friuliensis DSM 7358], AGZ41988	0	51%
17	1218	orf17	Unknown	hypothetical protein [Frigoribacterium sp. Leaf186], WP_056257329	3.0E-27	31%
18	195	orf18	Unknown	none		
19	594	orf19	Possible O-Me Transferase	caffeoyl-CoA O-methyltransferase [Actinopolyspora alba], SFE37636	1.0E-64	54%
20	495	orf20	Unknown	NUDIX pyrophosphate hydrolase [Kibdelosporangium aridum], WP_051897132	3.0E-72	85%

21	864	orf21	Possible N-acetyltransferase	N-acetyltransferase [Streptomyces yerevanensis], WP_033322847	7.0E-170	89%
22	405	orf22	Unknown	hypothetical protein [Kibdelosporangium aridum], WP_033390436	4.0E-75	83%
23	912	**mlcN**	Regulation	regulatory protein B [Streptomyces viridochromogenes], AEF16019	2.0E-122	61%
24	936	**mlcO**	Transport/Resistance	daunorubicin resistance protein DrrA family ABC transporter ATP-binding protein [Lechevalieria aerocolonigenes], WP_045314983	9.0E-125	70%
25	867	**mlcP**	4-Methylproline Biosynthesis	Coenzyme F420-dependent N5,N10-methylene tetrahydromethanopterin reductase [Streptomyces sp. WMMB 322], SCK14243	1.0E-72	47%
26	216	orf26	Unknown	none		
27	1086	**mlcQ**	4-Methylproline Biosynthesis	alcohol dehydrogenase [Streptomyces sp. CFMR 7], WP_053560816	1.0E-170	75%
28	801	**mlcR**	4-Methylproline Biosynthesis	L-proline 4-hydroxylase [Dactylosporangium sp.], BAA20094	2.0E-56	43%
29	2256	**mlcS**	2,3-Diaminobutyric Acid Biosynthesis	cysteine synthase [Saccharopolyspora spinosa], WP_010696131	0	64%
30	1722	**mlcT**	2,3-Diaminobutyric Acid Biosynthesis	argininosuccinate lyase, partial [Streptomyces sp. Termitarium-T10T-6], SCD57198	0	61%
31	267	**mlcU**	Regulation	LuxR family transcriptional regulator [Streptomyces sp. AW19M42], CEL20147	5.0E-46	93%
32	219	**mlcV**	Unknown NRPS function	MbtH family protein [Kibdelosporangium sp. MJ126-NF4], WP_042191548	9.0E-41	89%
33	546	orf33	Unknown	hypothetical protein [Kibdelosporangium sp. MJ126-NF4], WP_042191551	1.0E-51	74%
34	687	**mlcW**	Regulation	regulatory protein, tetR family [Amycolatopsis pretoriensis], SEF37903	8.0E-76	63%
35	795	orf35	Unknown	inositol monophosphatase [Kibdelosporangium sp. MJ126-NF4], WP_042191557	1.0E-143	76%
36	984	**mlcX**	Amino Acid Synthesis/Catabolism	L-asparaginase [Kibdelosporangium sp. MJ126-NF4], WP_042191561	4.0E-142	75%
37	3048	**mlcY**	Regulation	AfsR/SARP family transcriptional regulator [Kibdelosporangium sp. MJ126-NF4], WP_042191568	0	83%
38	1092	orf38	Unknown	hypothetical protein [Kibdelosporangium sp. MJ126-NF4], WP_042192840	0	77%
39	1383	orf39	Unknown	hypothetical protein [Kibdelosporangium phytohabitans], WP_054290662	0	77%

Table S2. Structures and ^{1}H and ^{13}C chemical shifts of malacidins A and B in D_2O[a]

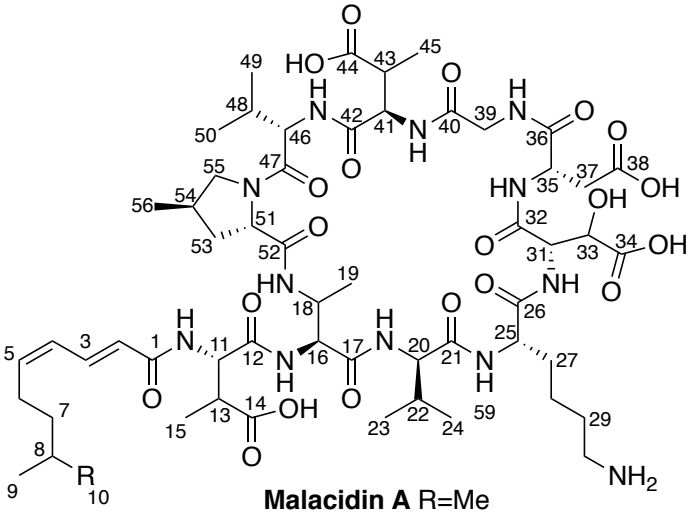

Malacidin A R=Me
Malacidin B R=Et

position		Malacidin A			Malacidin B		
		δ_C	δ_H mult. (*J* in Hz)		δ_C	δ_H mult. (*J* in Hz)	
atom	type	methyl-nonadienoic acid			methyl-decadienoic acid		
1	C	169.5			169.8		
2	CH	121.6	6.18	d (15.0)	121.7	6.19	d (15.0)
3	CH	138.1	7.64	dd (15.0, 11.0)	137.9	7.64	dd (15.0, 11.0)
4	CH	125.7	6.24	dd (11.0, 11.0)	125.8	6.25	dd (11.0, 11.0)
5	CH	143.3	6.03	ddd (11.0, 7.5, 7.5)	143.2	6.03	ddd (11.0, 7.5, 7.5)
6	CH_2	25.7	2.35	m	25.4	2.35	m
7	CH_2	37.9	1.33	m	35.5	1.45, 1.25	m
8	CH	27.0	1.58	m	33.3	1.38	m
9	CH_3	21.7	0.90	d (6.5)	18.4	0.89	d (6.5)
10	-	21.7	0.90	d (6.5)	28.7	1.36, 1.16	m
10-Me	CH_3				10.6	0.86	t (7.0)
				$_L$-MeAsp[1]			
11	CH	55.7	4.85	d (7.0)	57.1	4.67	m
12	C	172.6			173.7		
13	CH	40.5	3.13	m	42.4	2.94	m
14	C	177.4			180.3		
15	CH_3	12.4	1.23	d (7.0)	12.9	1.18	d (7.0)
				$_L$-MeDap[2]			
16	CH	58.1	4.53	d (3.5)	57.9	4.54	m
17	C	171.0			171.6		
18	CH	47.8	4.27	m	47.7	4.24	m
19	CH_3	15.7	1.24	d (6.5)	15.3	1.24	d (6.5)
				$_D$-Val[3]			
20	CH	57.3	4.38	m	57.3	4.35	d (8.0)
21	C	171.6			171.1		
22	CH	29.7	2.11	m	29.6	2.07	m
23	CH_3	17.7	0.97	m	17.7	1.00	m
24	CH_3	18.3	1.01	m	18.4	0.99	m
				$_L$-Lys[4]			
25	CH	53.1	4.43	dd (10.0, 5.0)	53.0	4.48	dd (7.5, 6.0)
26	C	173.8			173.5		
27	CH_2	30.1	1.94, 1.79	m	30.4	1.92, 1.83	m

28	CH_2	22.1	1.49, 1.44	m	21.8	1.45, 1.45	m
29	CH_2	26.1	1.71, 1.71	m	26.2	1.72, 1.72	m
30	CH_2	39.0	3.02, 3.02	t (7.5)	39.0	3.02, 3.02	m
				$_L$-HyAsp[5]			
31	CH	56.6	4.68	d (5.5)	57.4	4.62	d (4.5)
32	C	169.9			170.1		
33	CH	70.5	4.58	d (5.5)	72.2	4.34	d (4.5)
34	C	174.5			176.6		
				$_L$-Asp[6]			
35	CH	49.8	4.81	overlapped	51.0	4.69	m
36	C	172.4			173.4		
37	CH_2	35.0	2.94, 2.94	dd (13.0, 6.5)	37.5	2.74, 2.74	m
38	C	174.2			177.3		
				Gly[7]			
39	CH_2	42.6	3.98, 3.98	s	42.4	4.03, 3.93	d (17.0)
40	C	171.0			170.7		
				$_D$-MeAsp[8]			
41	CH	54.9	4.70	d (7.5)	56.1	4.55	m
42	C	171.4			172.1		
43	CH	40.7	3.06	m	43.3	2.79	m
44	C	177.4			180.5		
45	CH_3	13.4	1.21	d (7.5)	14.2	1.13	d (7.0)
				$_L$-Val[9]			
46	CH	60.3	4.03	d (8.0)	60.2	4.08	d (8.0)
47	C	173.3			172.7		
48	CH	29.3	2.12	m	29.6	2.17	m
49	CH_3	18.5	0.98	d (7.0)	18.5	0.96	m
50	CH_3	18.1	0.97	d (6.5)	18.1	0.98	m
				$_L$-MePro[10]			
51	CH	60.3	4.39	m	60.2	4.41	dd (8.0, 5.5)
52	C	173.8			174.1		
53	CH_2	36.4	1.96, 1.86	m	36.5	1.93, 1.89	m
54	CH	32.2	2.48	m	32.2	2.45	m
55	CH_2	54.6	3.79, 3.43	t (9.0, 6.5)	54.6	3.79, 3.43	m
56	CH_3	16.8	1.01	d (6.5)	16.8	1.00	m

[a] ^1H and ^{13}C NMR were obtained at 600 and 150 MHz, respectively. These chemical shifts are representative of 4 independent fermentations and isolations of malacidin, and were referenced to the methyl group of triethylamine in D_2O (δ_C 8.189, δ_H 1.292). The triethylamine concentrations in D_2O are 3.59mM for malacidins A and B. Each molar concentration of malacidins A and B was 11.21mM and 7.92mM.

Table S3. Results of Marfey's Analysis of malacidin A and B.

Amino acids of malacidin A	t_{RL} (min)	t_{RD} (min)	Elution order	Δt (t_{RD}-t_{RL}, min)
$_D$-valine	27.1	22.2	D → L	-4.9
$_L$-lysine(di)	28.7	30.6	L → D	1.9
$_L$-hydroxyl aspartic acid	16.0	15.0	D → L	-1.0
$_L$-aspartic acid	13.4	14.4	L → D	1.0
$_L$-valine	22.3	27.0	L → D	4.7
$_L$-(4*R*) methyl proline	21.2	22.7	L → D	1.5
(2*S*,4*R*)-4-methylpyrrolidine-2-carboxylic acid	20.9	22.4	L → D	1.5

Amino acids of malacidin B	t_{RL} (min)	t_{RD} (min)	Elution order	Δt (t_{RD}-t_{RL}, min)
$_D$-valine	27.0	22.2	D → L	-4.8
$_L$-lysine(di)	28.8	30.9	L → D	2.1
$_L$-hydroxyl aspartic acid	14.7	14.4	D → L	-0.3
$_L$-aspartic acid	13.0	14.3	L → D	1.3
$_L$-valine	22.2	26.9	L → D	4.7
$_L$-(4*R*) methyl proline	21.2	22.6	L → D	1.4

Table S4. Full Spectrum of Activity of Malacidin Antibiotics and Daptomycin. The values in the table are representative of the range of MICs determined in at least three independent experiments.

Organism		Acquired Resistance	Malacidin A MIC (μg mL^{-1})	Malacidin B MIC (μg mL^{-1})	Daptomycin MIC (μg mL^{-1})
Acinetobacter baumannii	ATCC 17978		>100	>100	>100
Bacillus subtilis	168 IAI		0.2-0.4	N.D.	0.2-0.4
Candida albicans	ATCC 1884		>100	>100	>100
Cryptococcus neoformans	ATCC 32045		>100	>100	>100
Enterococcus faecium	Com15		0.8-2.0	0.8-2.0	0.4-2.0
Enterococcus faecium	VRE	Vancomycin (VRE)	0.8-2.0	N.D.	0.4-2.0
Escherichia coli	DH5α		>100	>100	>100
Escherichia coli	BAS849		>100	N.D.	50-100
Human embryonic kidney cells	HEK293		>100[a]	N.D.	>100[a]
Human lung fibroblast cells	MRC5		>100[a]	N.D.	N.D.
Klebsiella pneumonia	ATCC 10031		>100	>100	>100
Lactobacillus rhamnosus	NCTC 13031		0.1-0.2	N.D.	N.D.
Pseudomonas aeruginosa	PAO1		>100	>100	>100
Salmonella enterica	IR 715		>100	>100	>100
Staphylococcus aureus	USA300	β-lactams (Methicillin, Oxacillin, Penicillin)	0.2-0.8	0.4-0.8	0.2-0.8
Staphylococcus aureus + 10 % Serum	USA300	β-lactams (Methicillin, Oxacillin, Penicillin)	0.2-0.8	N.D.	N.D.
Staphylococcus aureus	COL	β-lactams (Methicillin, Oxacillin, Penicillin)	0.2-0.8	N.D.	0.2-0.8
Staphylococcus aureus	BAA-42	β-lactams (Methicillin, Oxacillin, Penicillin)	0.2-0.8	N.D.	0.2-0.8
Staphylococcus aureus	NRS100	β-lactams, Tetracycline	0.2-0.8	N.D.	0.2-0.8
Staphylococcus aureus	NRS108	β-lactams, Gentamicin, Kanamycin	0.2-0.8	N.D.	0.2-0.8
Staphylococcus aureus	NRS140	β-lactams, Erythromycin, Spectinomycin	0.4-2.0	N.D.	0.2-0.8
Staphylococcus aureus	NRS146	β-lactams, Vancomycin (VISA)	0.4-0.8	N.D.	0.2-0.8
Streptococcus mutans	UA159		0.1-0.2	N.D.	N.D.
Streptococcus pneumoniae	TCH8431		0.1-0.2	N.D.	0.1-0.2

N.D. = Not determined/Tested
[a] = Viability assessed by ATP release assay

Figure S1. Additional bioinformatic analysis of calcium-dependent antibiotics. (a) Phylogenetic trees of NRPS AD domains from known reference calcium-dependent antibiotic BGCs using *i)* all NRPS AD domains, *ii)* Asp4 NRPS AD domains only, *iii)* Asp4 NRPS AD domains from references and Asp4-like eSNAPD-processed NRPS AD domains from soil metagenomes. Phylogenetic trees including soil metagenomes NRPS AD domains with hits for Asp6 and Gly7 in the calcium-dependent DXDG motif are included in **(b)** and **(c)**, respectively. **(d)** Geospatial distributions of specific molecule NPSTs from screened soil metagenomes.

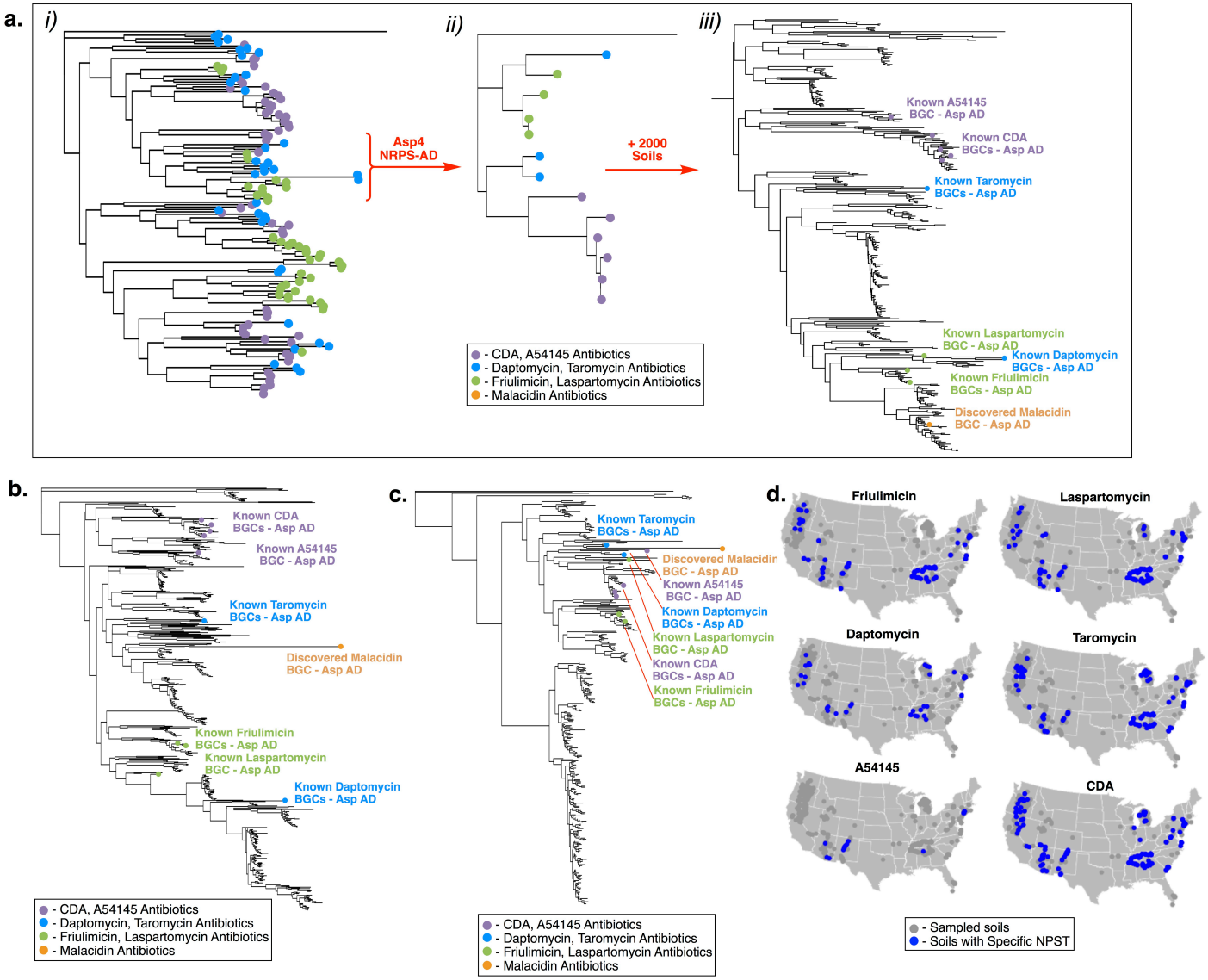

Figure S2. ^{1}H NMR spectrum of malacidin A in D_2O. Representative NMR spectrum of malacidin from 4 independent fermentations and isolations.

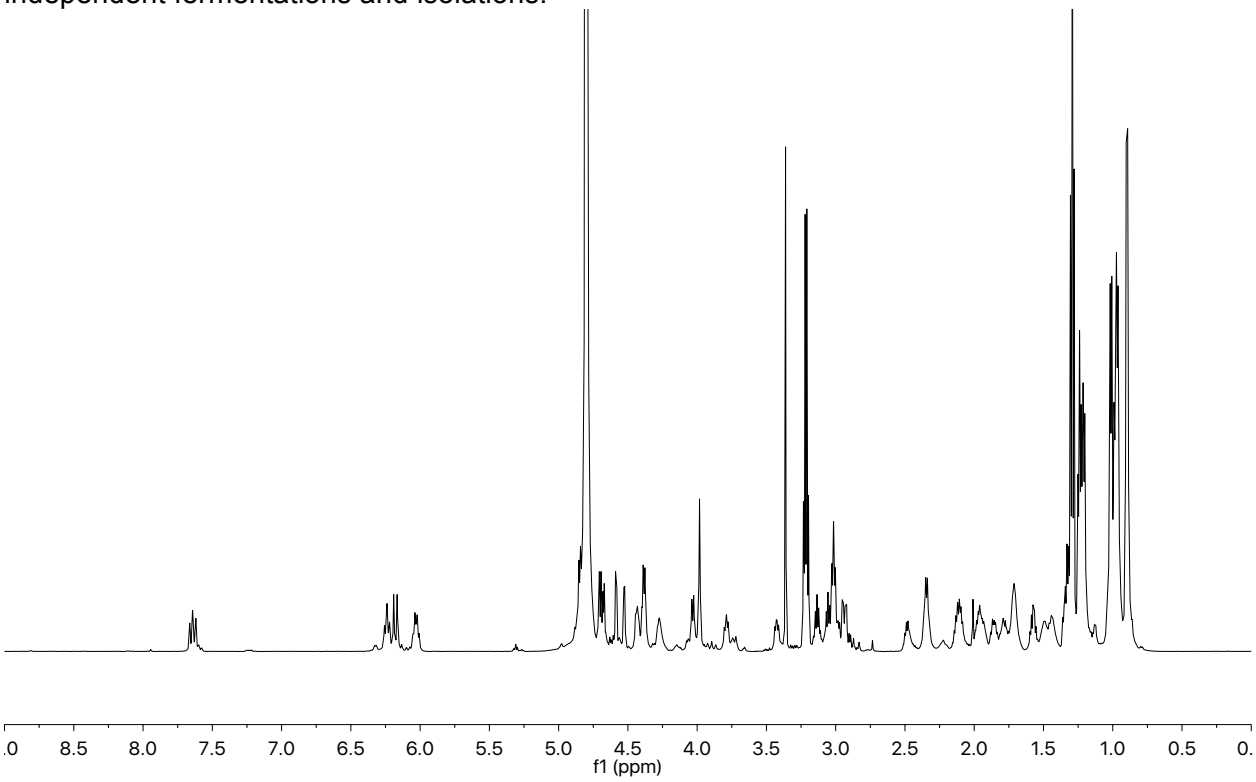

Figure S3. ^{13}C NMR spectrum of malacidin A in D_2O. Representative NMR spectrum of malacidin from 4 independent fermentations and isolations. Chemical shifts of trifluoroacetic acid are indicated by an X.

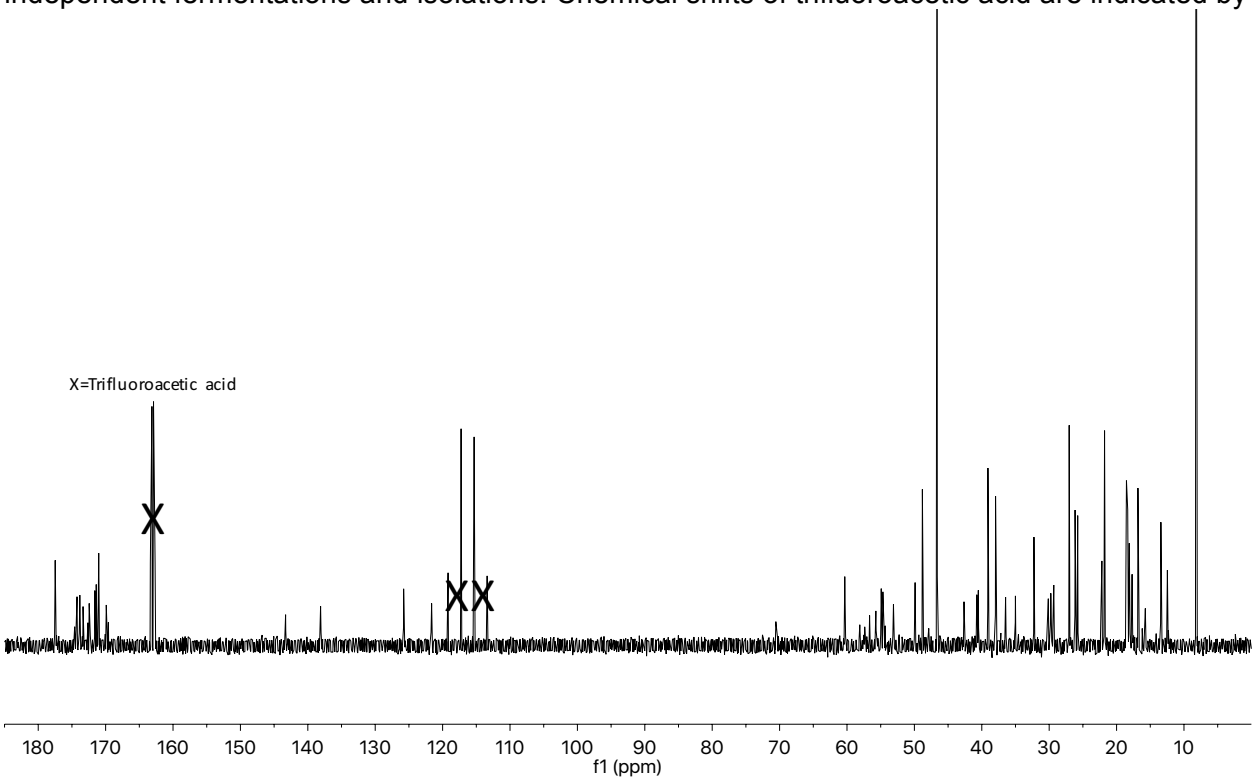

Figure S4. HSQC NMR spectrum of malacidin A. Representative NMR spectrum of malacidin from 4 independent fermentations and isolations.

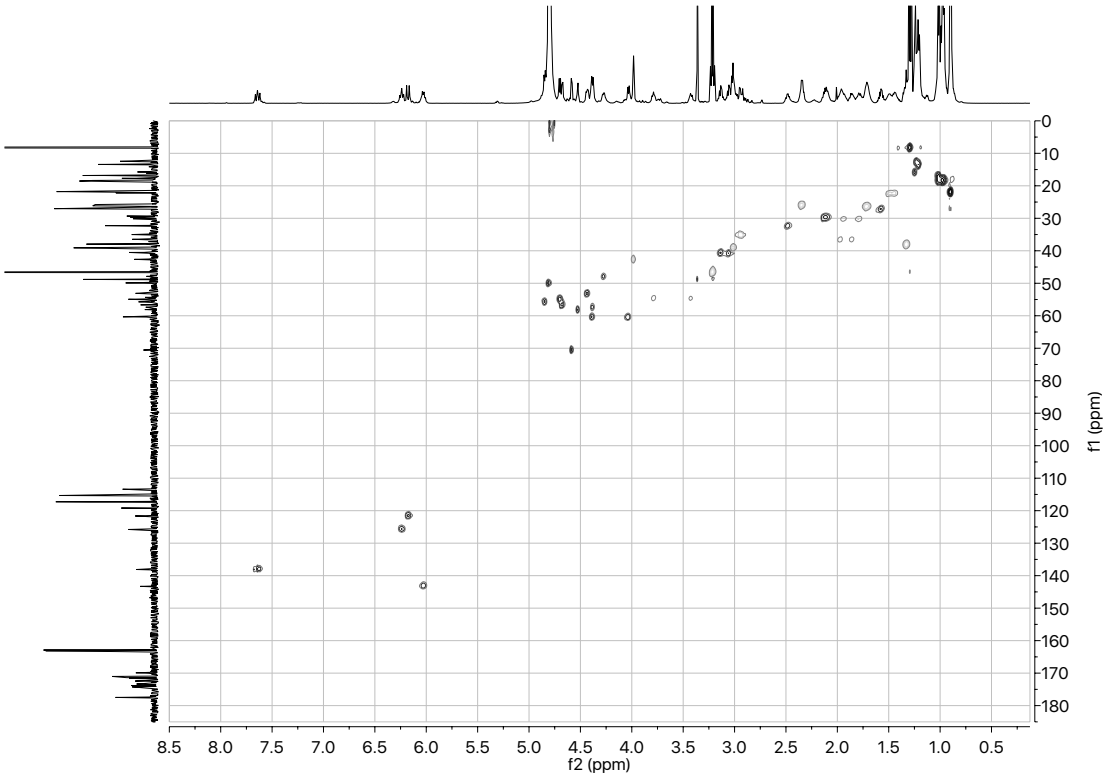

Figure S5. COSY NMR spectrum of malacidin A. Representative NMR spectrum of malacidin from 4 independent fermentations and isolations.

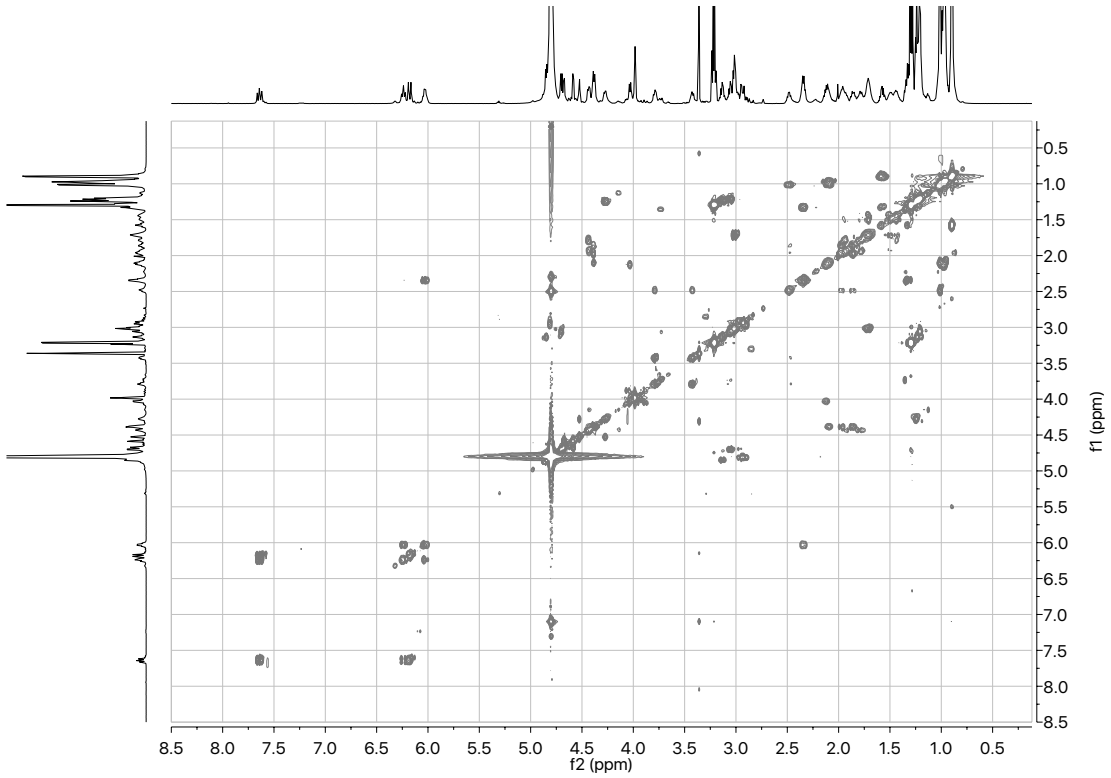

Figure S6. TOCSY NMR spectrum of malacidin A. Representative NMR spectrum of malacidin from 4 independent fermentations and isolations.

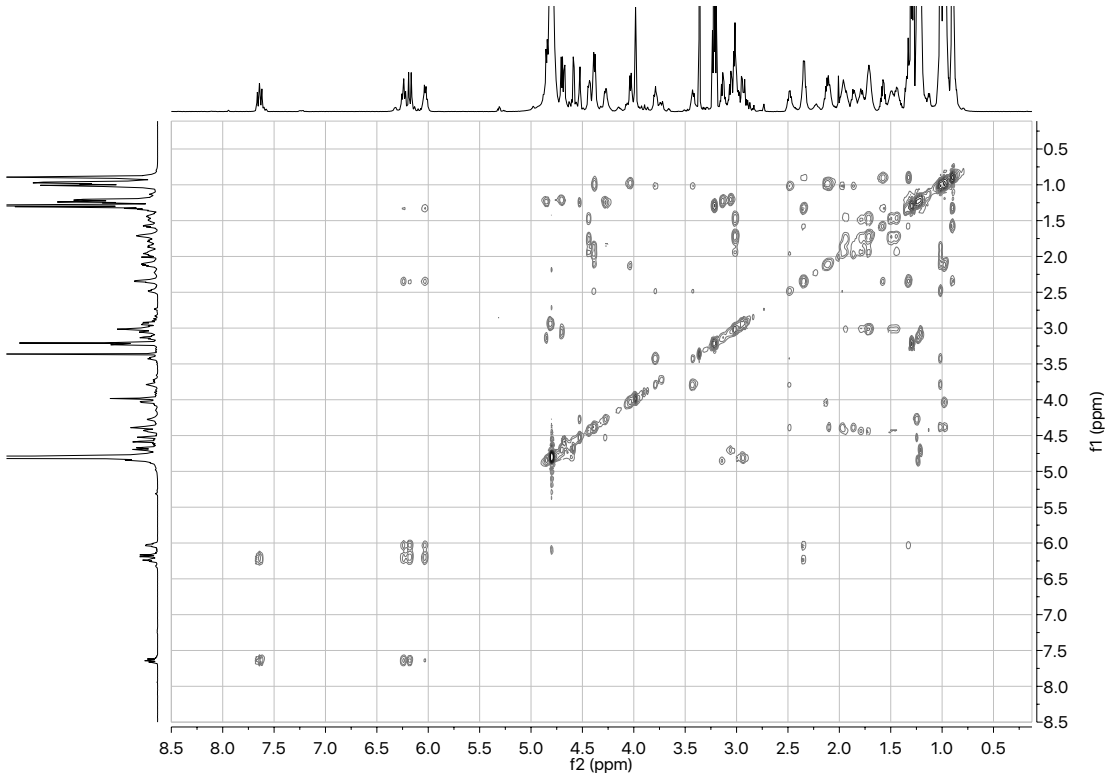

Figure S7. HMBC NMR spectrum of malacidin A. Representative NMR spectrum of malacidin from 4 independent fermentations and isolations.

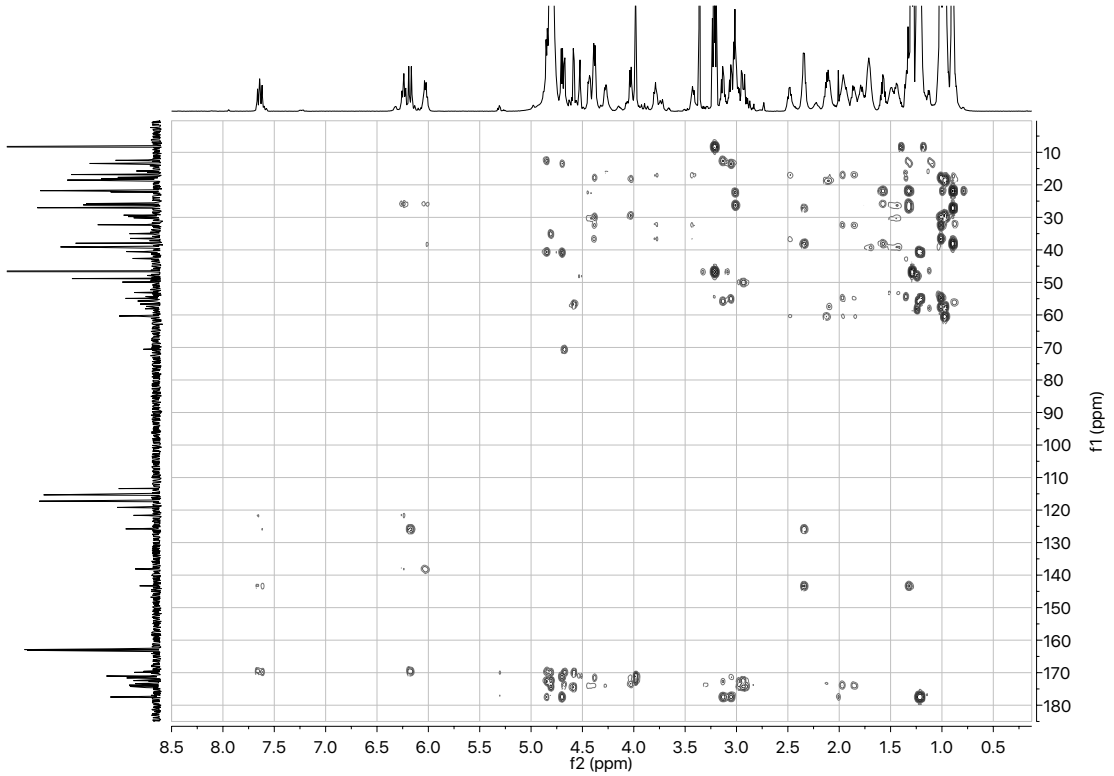

Figure S8. ^{1}H NMR spectrum of malacidin B in D_2O. Representative NMR spectrum of malacidin from 4 independent fermentations and isolations.

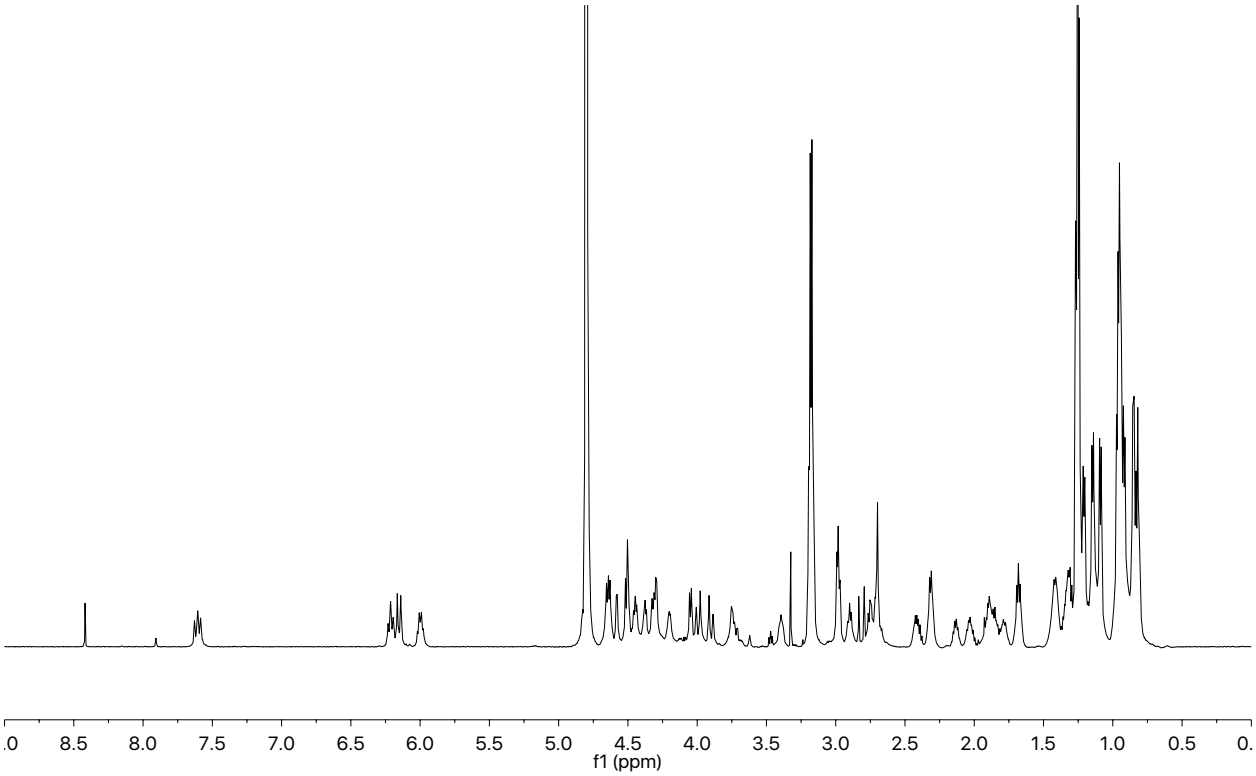

Figure S9. ^{13}C NMR spectrum of malacidin B in D_2O. Representative NMR spectrum of malacidin from 4 independent fermentations and isolations. Chemical shifts of trifluoroacetic acid are indicated by an X.

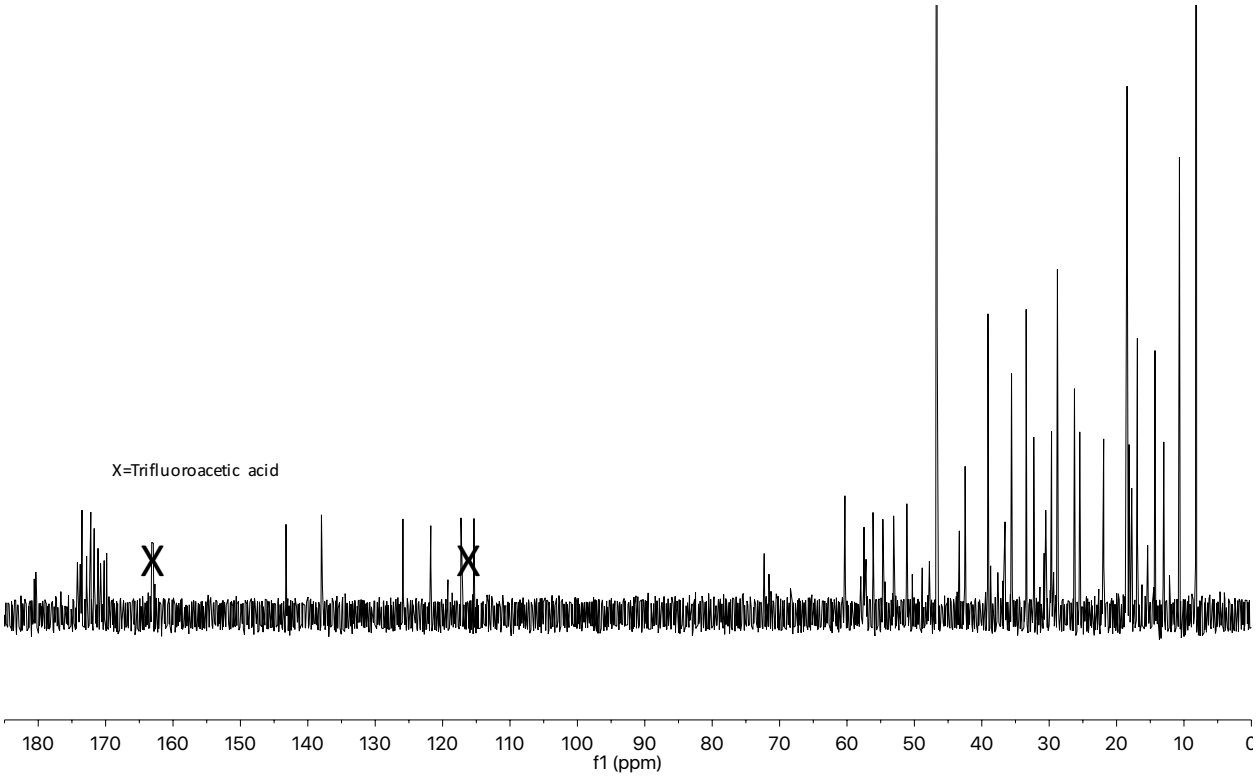

Figure S10. HSQC NMR spectrum of malacidin B. Representative NMR spectrum of malacidin from 4 independent fermentations and isolations.

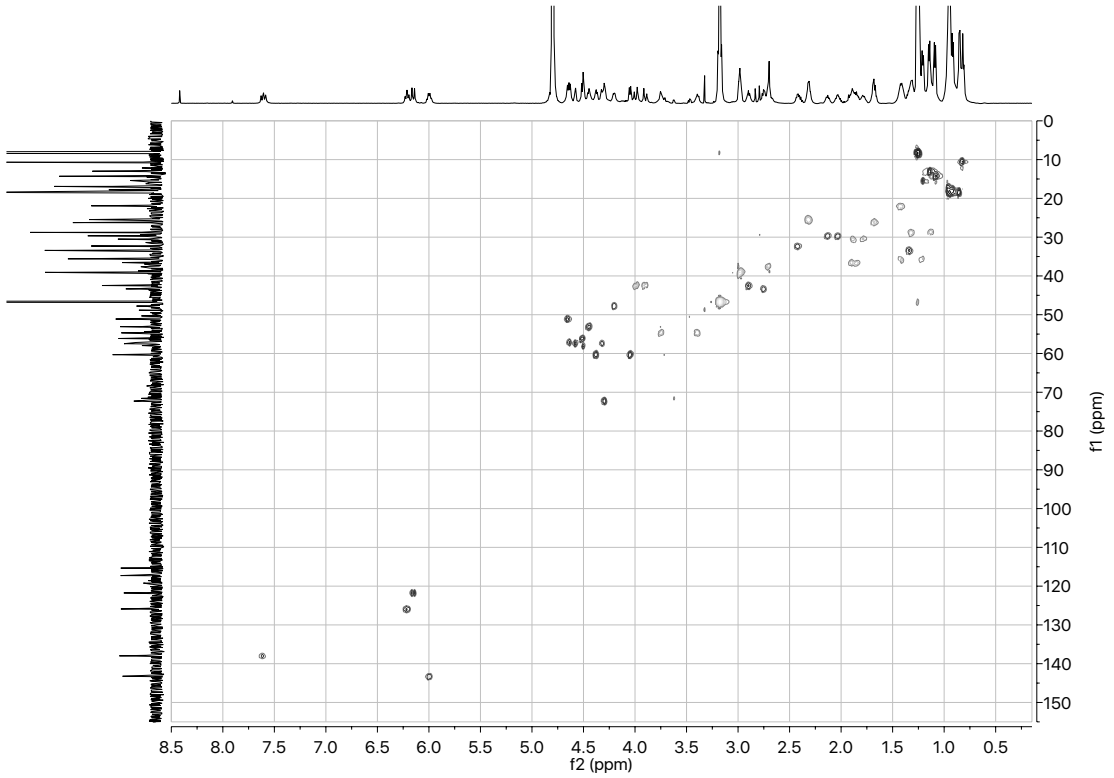

Figure S11. COSY NMR spectrum of malacidin B. Representative NMR spectrum of malacidin from 4 independent fermentations and isolations.

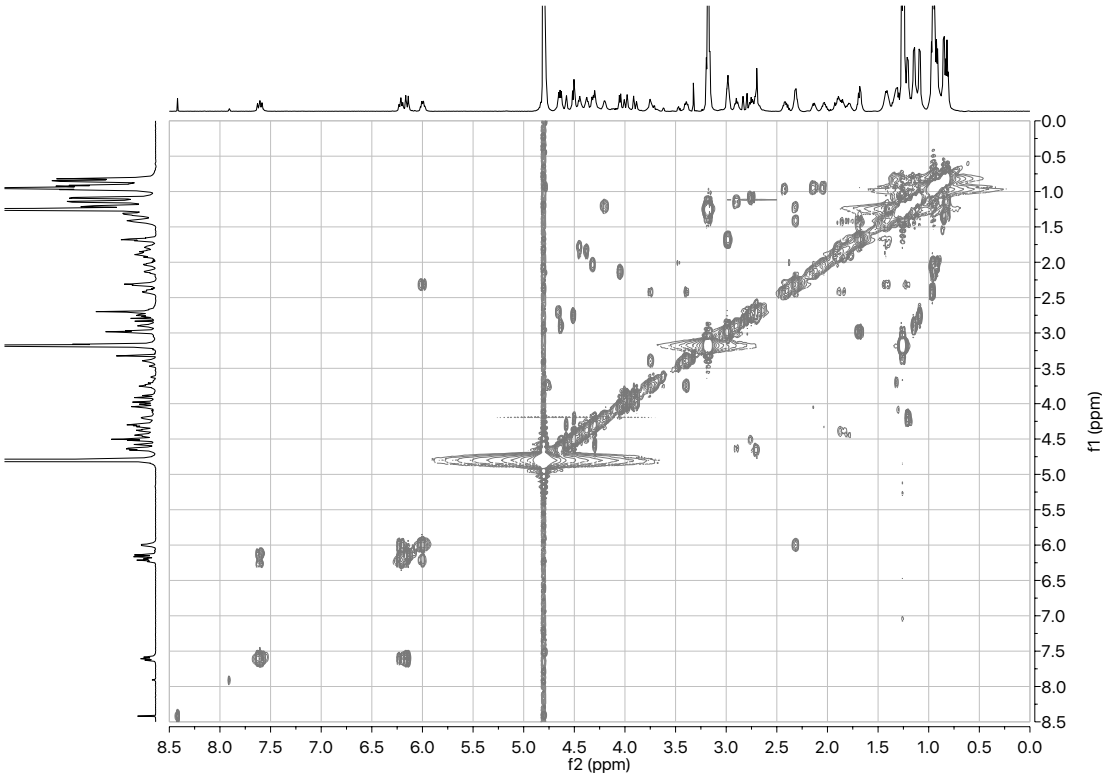

Figure S12. TOCSY NMR spectrum of malacidin B. Representative NMR spectrum of malacidin from 4 independent fermentations and isolations.

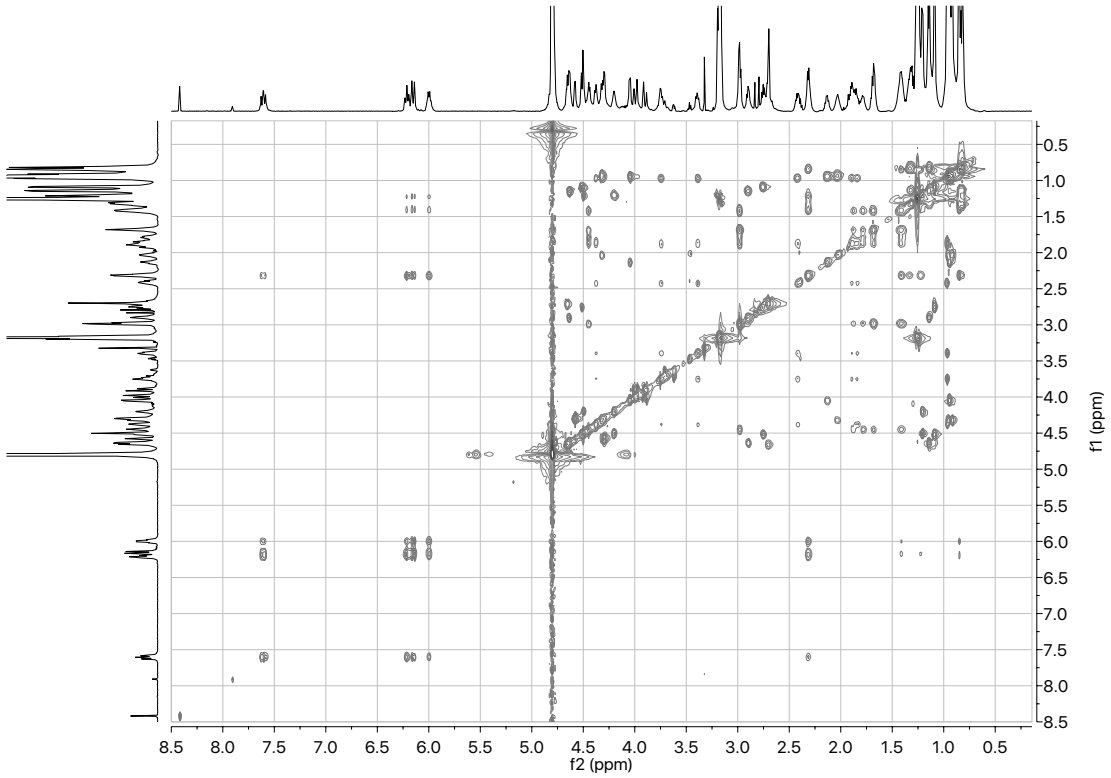

Figure S13. HMBC NMR spectrum of malacidin B. Representative NMR spectrum of malacidin from 4 independent fermentations and isolations.

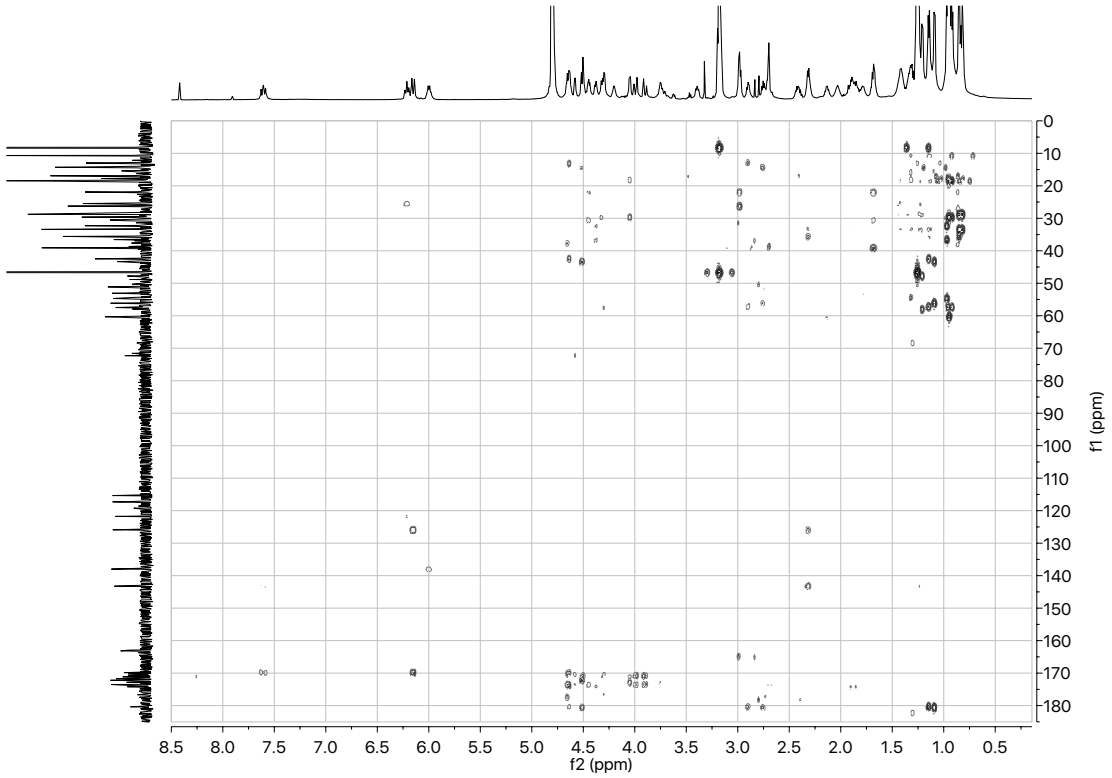

Figure S14. The partial structures of malacidin A from NMR analysis.
(a) Each amino acid unit and fatty acid side chain were developed by COSY, TOCSY, and HMBC correlations. **(b)** The key correlations between α protons of amino acid units and carbonyl carbons. Based on this data, five partial structures were determined.

a

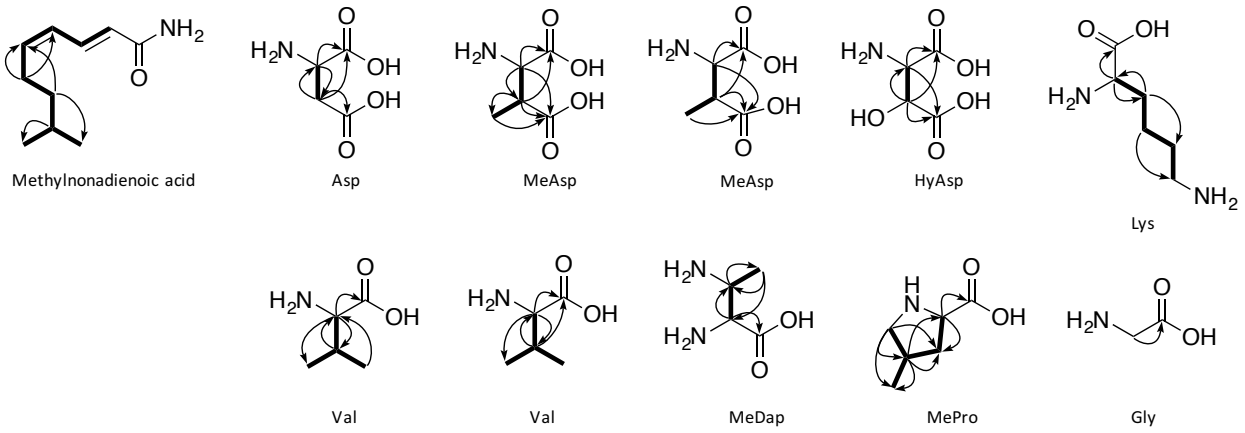

b

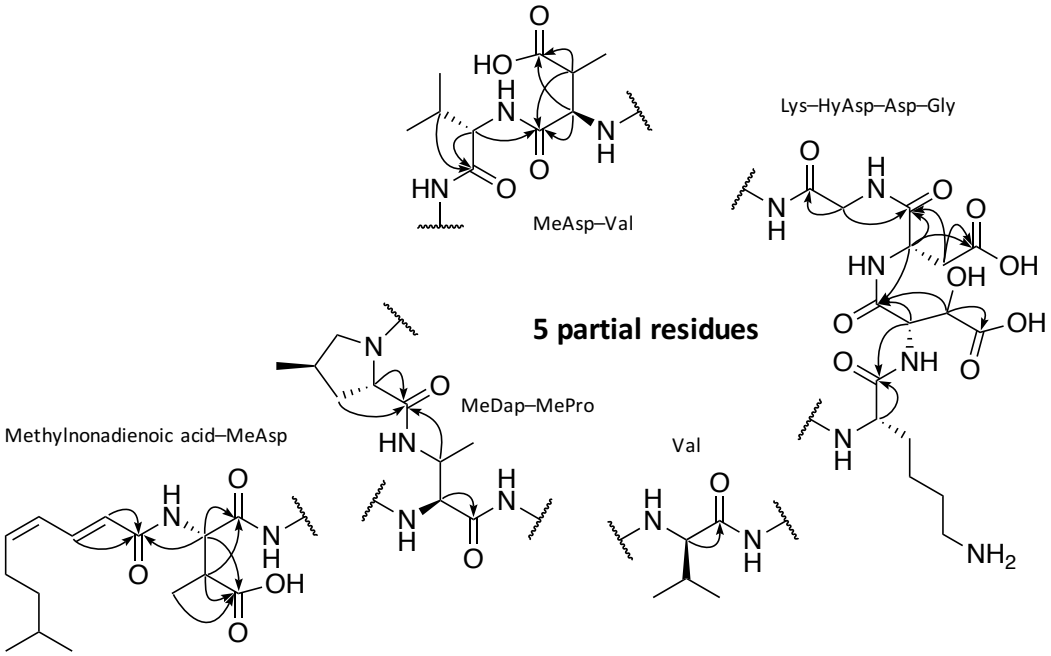

Figure S15. ESI-MS/MS fragmentation patterns of propionate malacidin A. (a) For MS/MS analysis, the malacidins were reacted with propionic anhydride. **(b)** Five partial residues, which were determined from NMR, were connected by MS/MS fragmentation major ion (highlighted in bold text). The MS spectrum is representative across two independent derivatizations and MS analysis. **(c)** The sequential MS/MS fragmentation of malacidin A and B begins with the loss of Val between the MePro and MeAsp. The mass malacidin after the loss of each sequential residue is indicated and fragment units are noted by color. Other major MS/MS fragments present in (b) are MeAsp-Gly-Asp-HyAsp (*) and the 9-mer cyclic peptide core (#).

a.

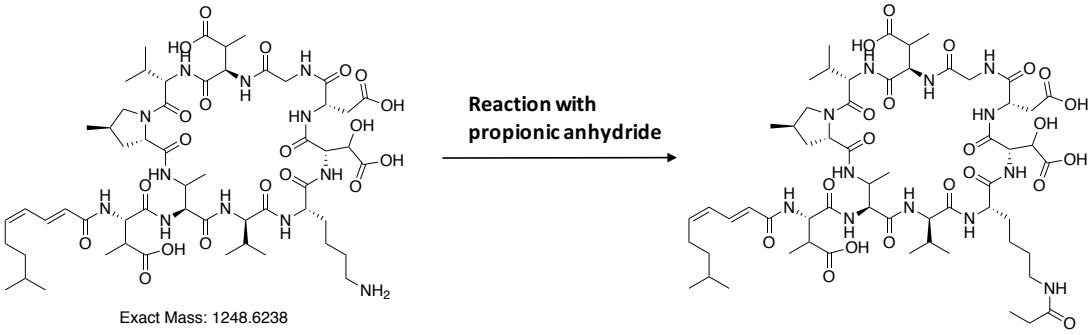

b.

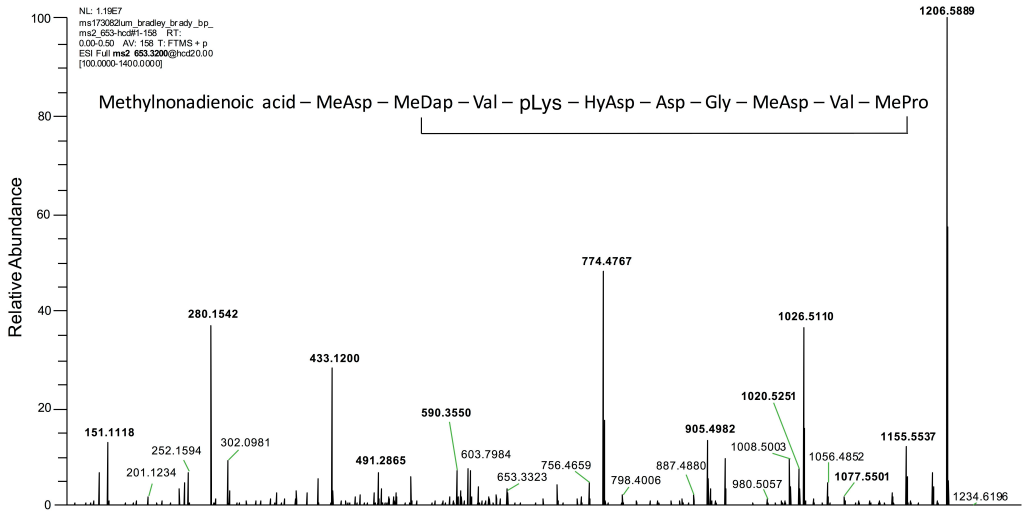

c.

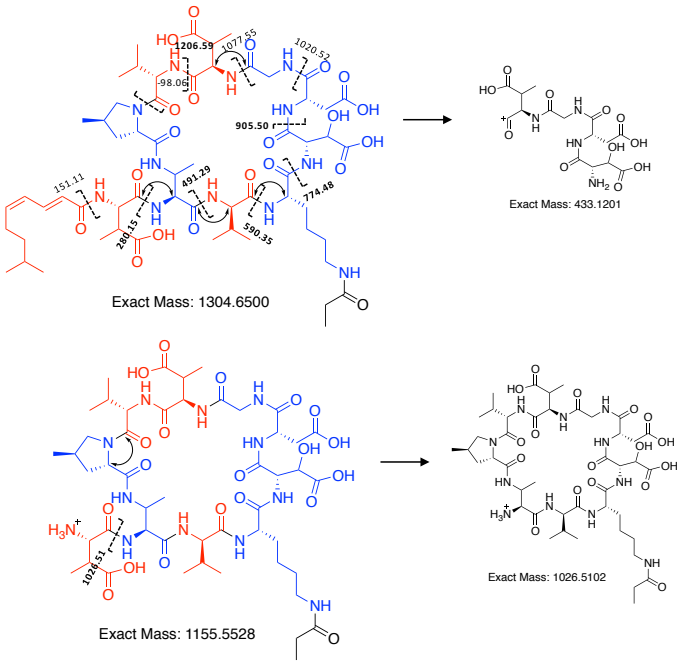

Figure S16. Comparison of MS/MS fragmentation patterns of propionate malacidins A and B. Red labeled exact mass ions were originated from the core cyclic peptide of malacidins A and B. Spectra are representative across two independent derivatizations and MS analysis.

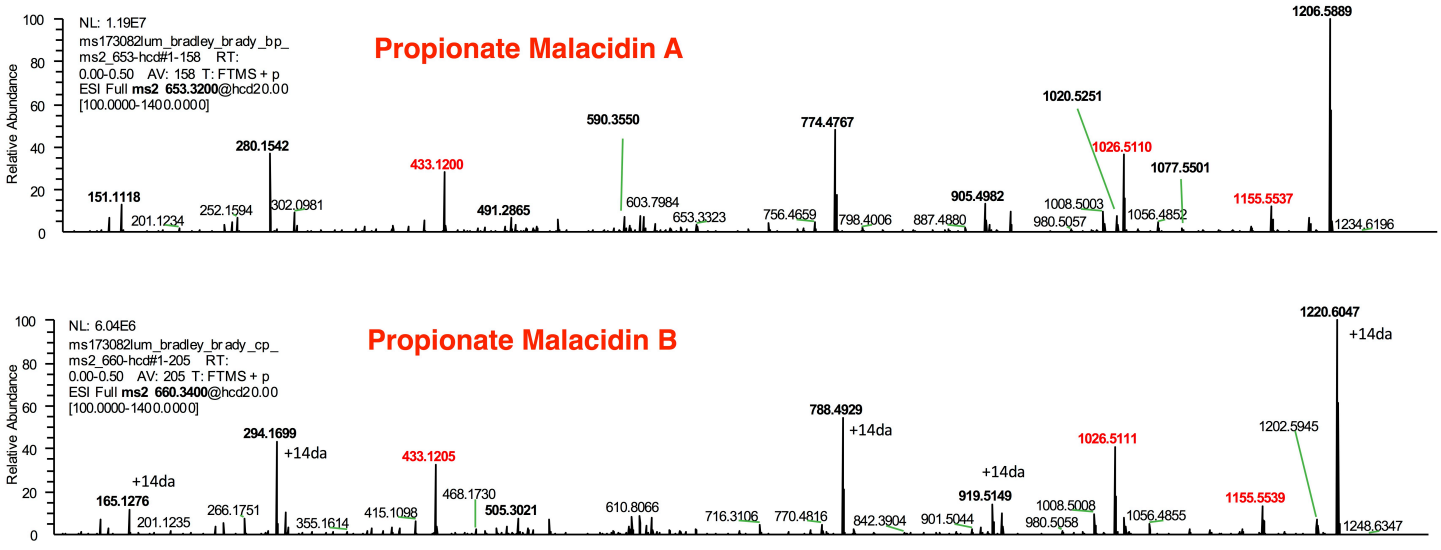

Figure S17. The key HMBC and COSY correlations of malacidin A.

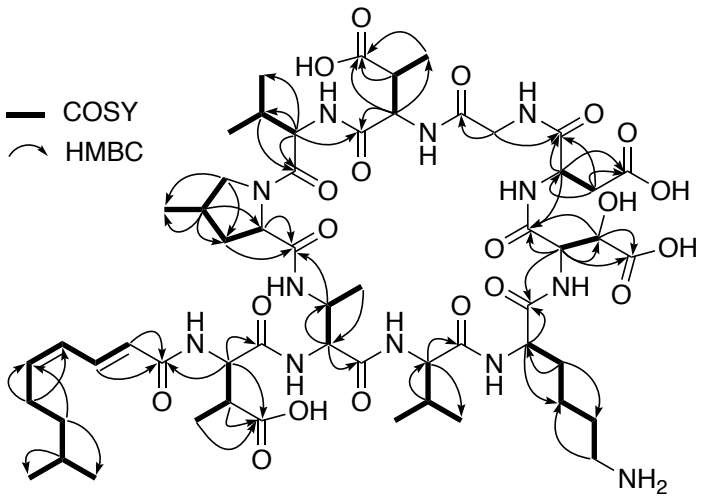

Figure S18. The key HMBC and COSY correlations of malacidin B.

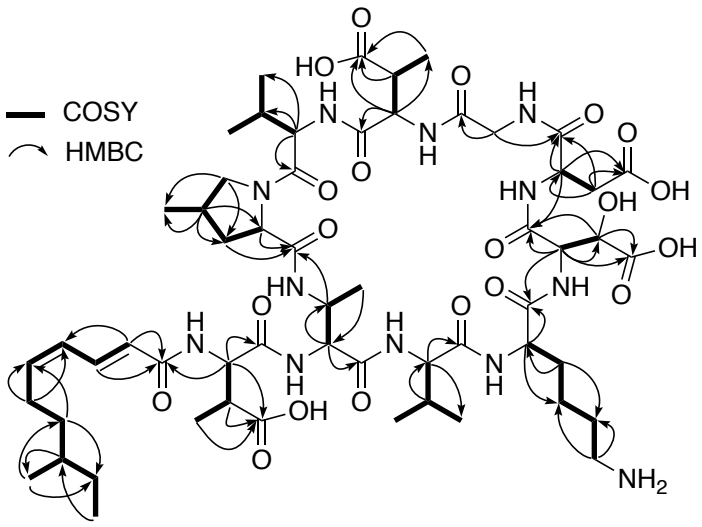

Figure S19. ROESY NMR spectrum of malacidin A. Representative NMR spectrum of malacidin from 4 independent fermentations and isolations. Key correlations are highlighted in the red box, and zoomed in below the main spectrum.

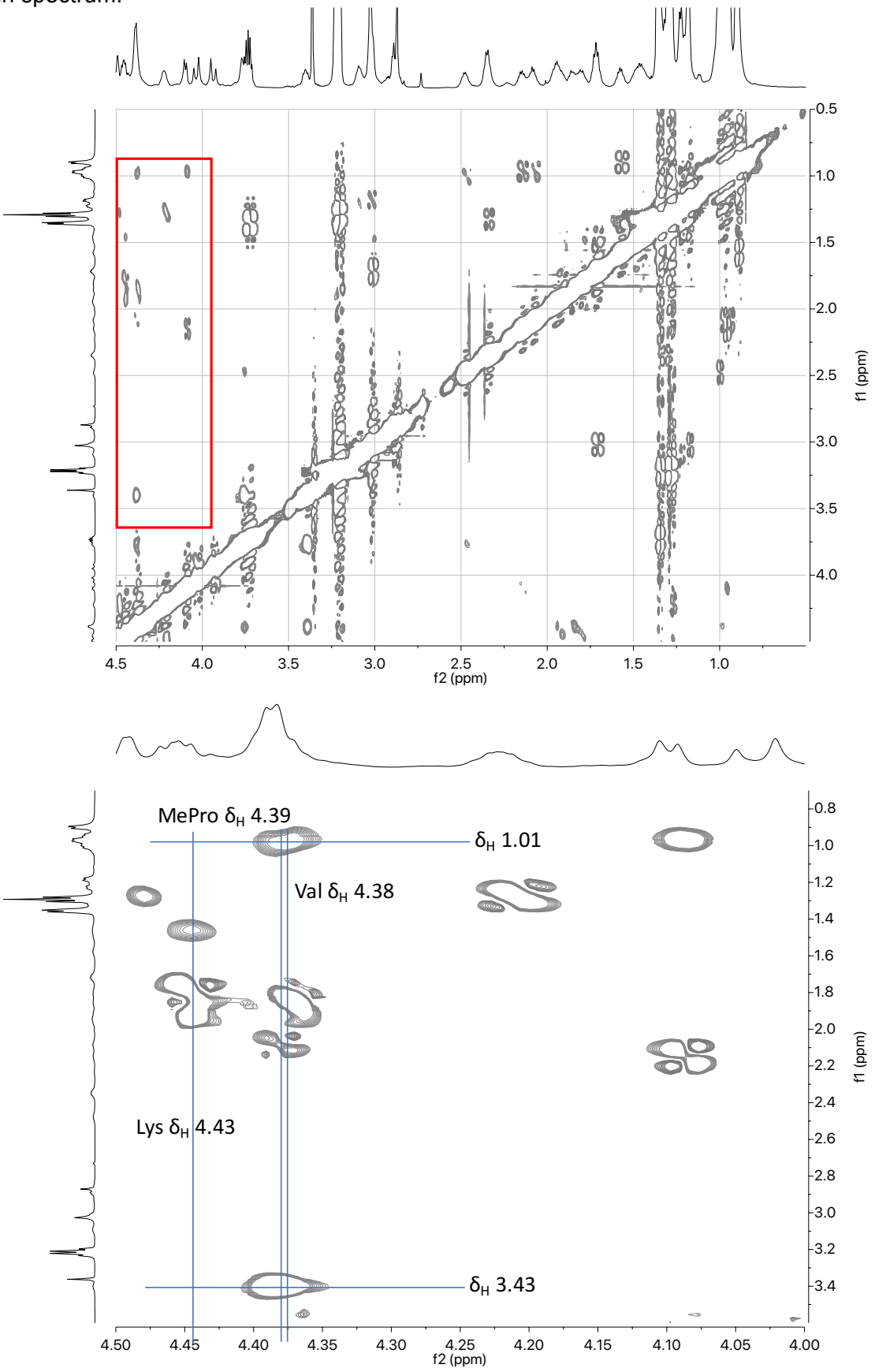

Figure S20. The key ROESY correlations of methyl proline of malacidin A.

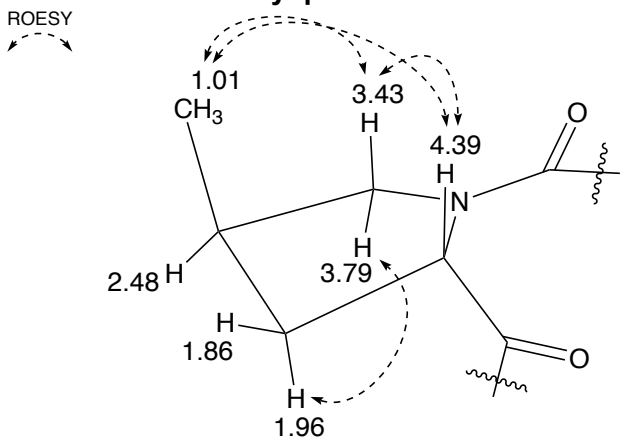

Figure S21. LC-MS charts of $_{L, D}$-FDAA derivatives of malacidin A. Chromatograms are representative across two independent derivatizations.

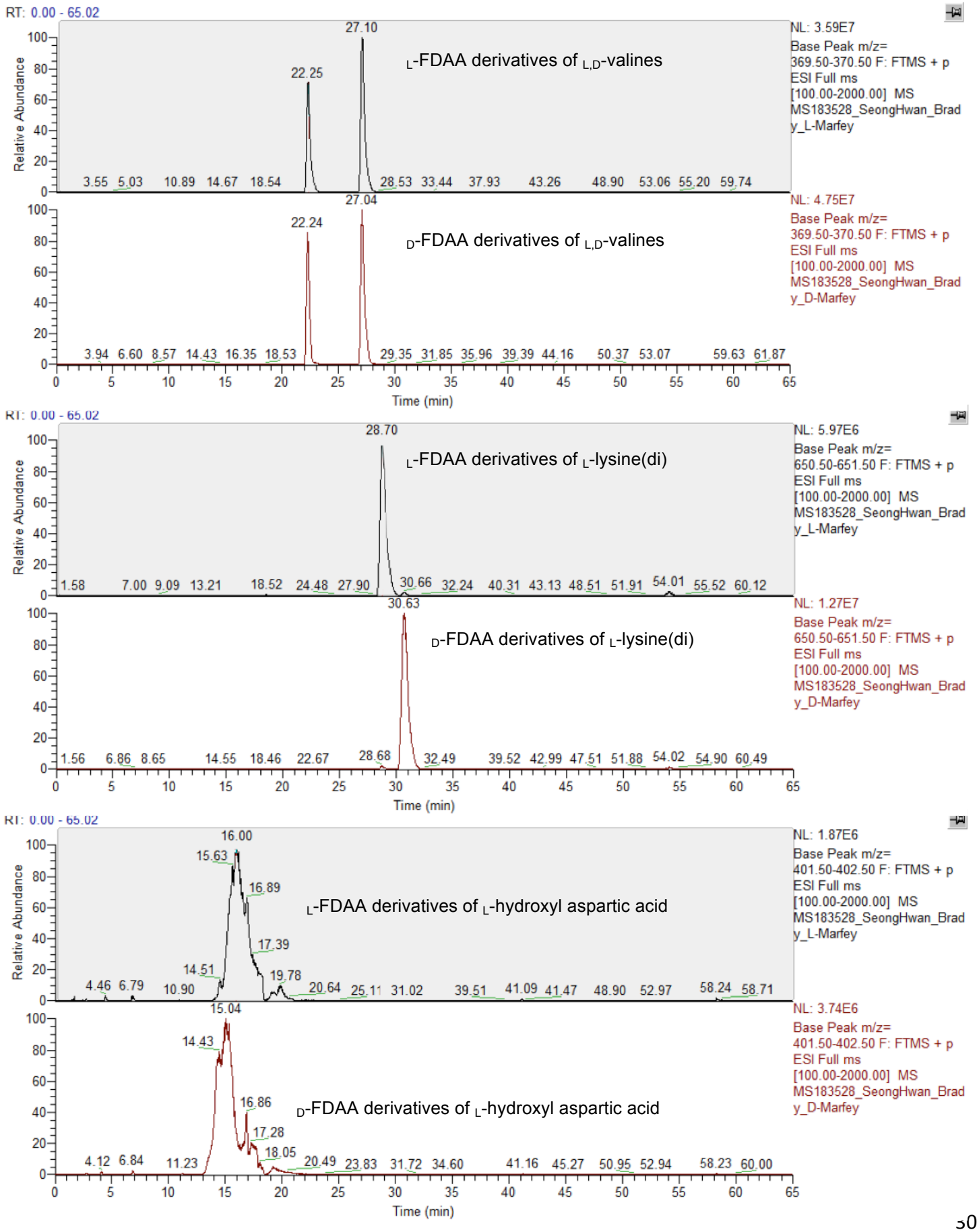

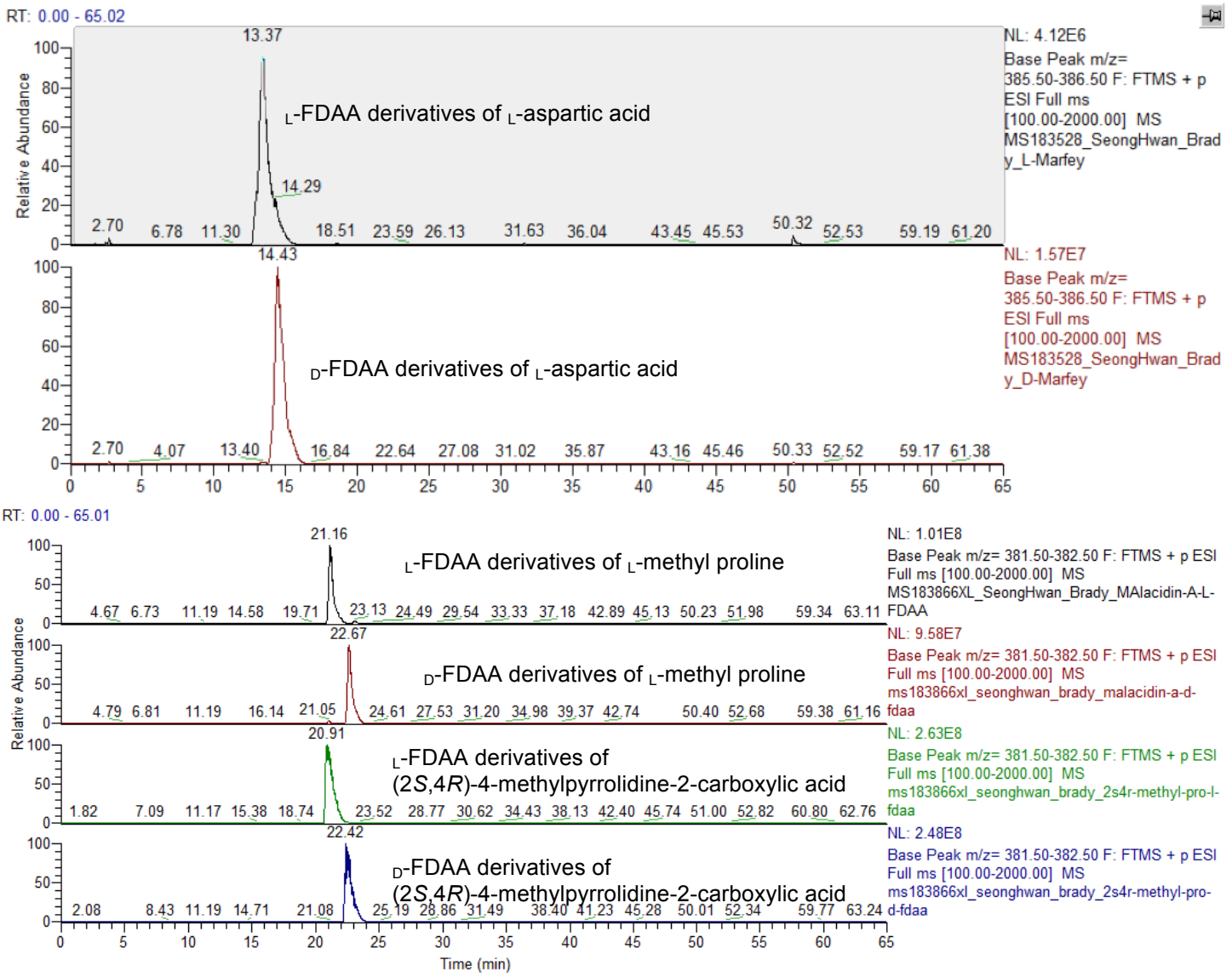
RT: 0.00 - 65.02
Relative Abundance
13.37
L-FDAA derivatives of L-aspartic acid
14.29
NL: 4.12E6
Base Peak m/z= 385.50-386.50 F: FTMS + p ESI Full ms [100.00-2000.00] MS MS183528_SeongHwan_Brady_L-Marfey
14.43
D-FDAA derivatives of L-aspartic acid
NL: 1.57E7
Base Peak m/z= 385.50-386.50 F: FTMS + p ESI Full ms [100.00-2000.00] MS MS183528_SeongHwan_Brady_D-Marfey
RT: 0.00 - 65.01
21.16
L-FDAA derivatives of L-methyl proline
NL: 1.01E8
Base Peak m/z= 381.50-382.50 F: FTMS + p ESI Full ms [100.00-2000.00] MS MS183866XL_SeongHwan_Brady_MAlacidin-A-L-FDAA
22.67
D-FDAA derivatives of L-methyl proline
NL: 9.58E7
Base Peak m/z= 381.50-382.50 F: FTMS + p ESI Full ms [100.00-2000.00] MS ms183866xl_seonghwan_brady_malacidin-a-d-fdaa
20.91
L-FDAA derivatives of (2S,4R)-4-methylpyrrolidine-2-carboxylic acid
NL: 2.63E8
Base Peak m/z= 381.50-382.50 F: FTMS + p ESI Full ms [100.00-2000.00] MS ms183866xl_seonghwan_brady_2s4r-methyl-pro-l-fdaa
22.42
D-FDAA derivatives of (2S,4R)-4-methylpyrrolidine-2-carboxylic acid
NL: 2.48E8
Base Peak m/z= 381.50-382.50 F: FTMS + p ESI Full ms [100.00-2000.00] MS ms183866xl_seonghwan_brady_2s4r-methyl-pro-d-fdaa
Time (min)

Figure S22. LC-MS charts of $_{L, D}$-FDAA derivatives of malacidin B. Chromatograms are representative across two independent derivatizations.

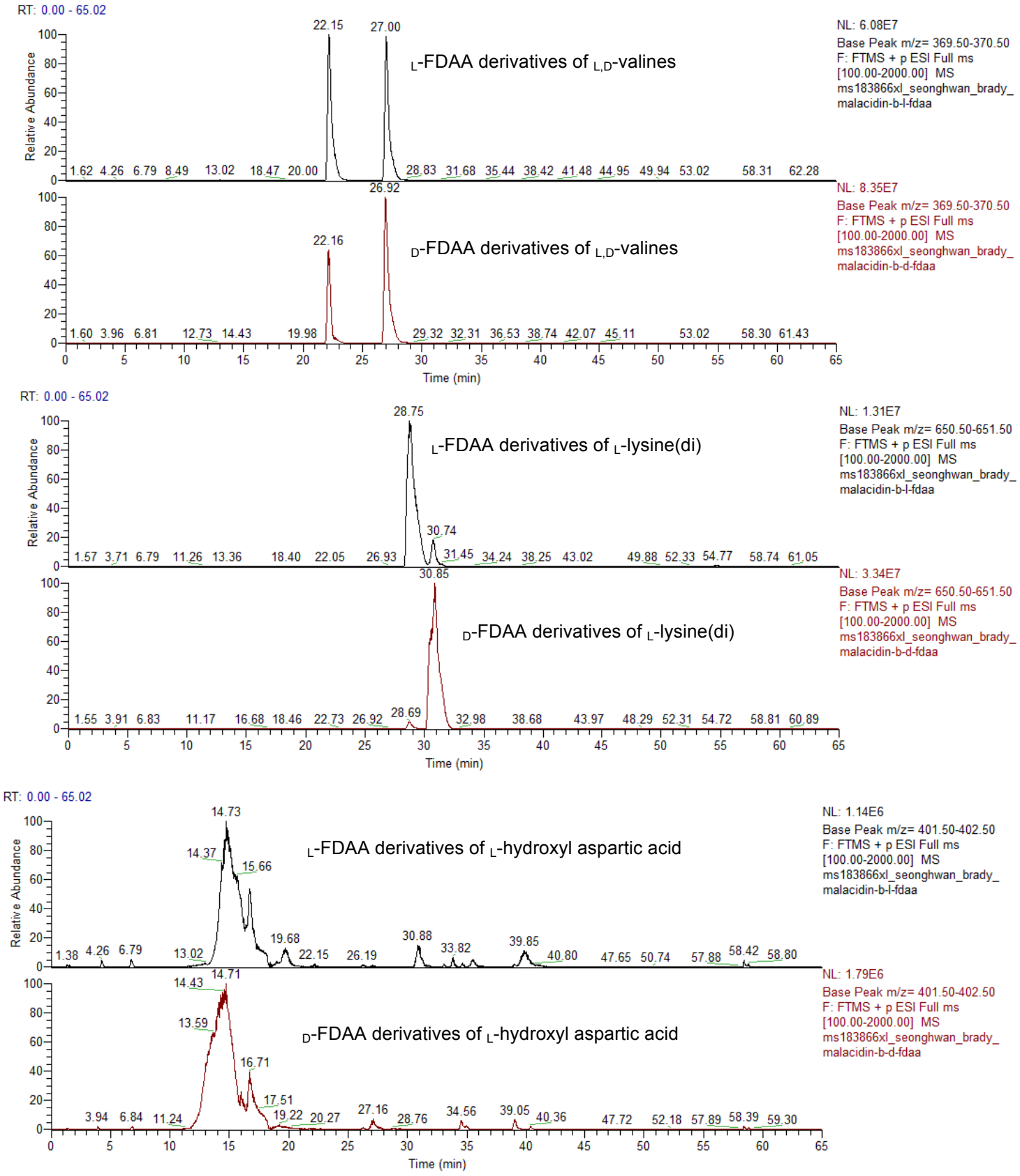

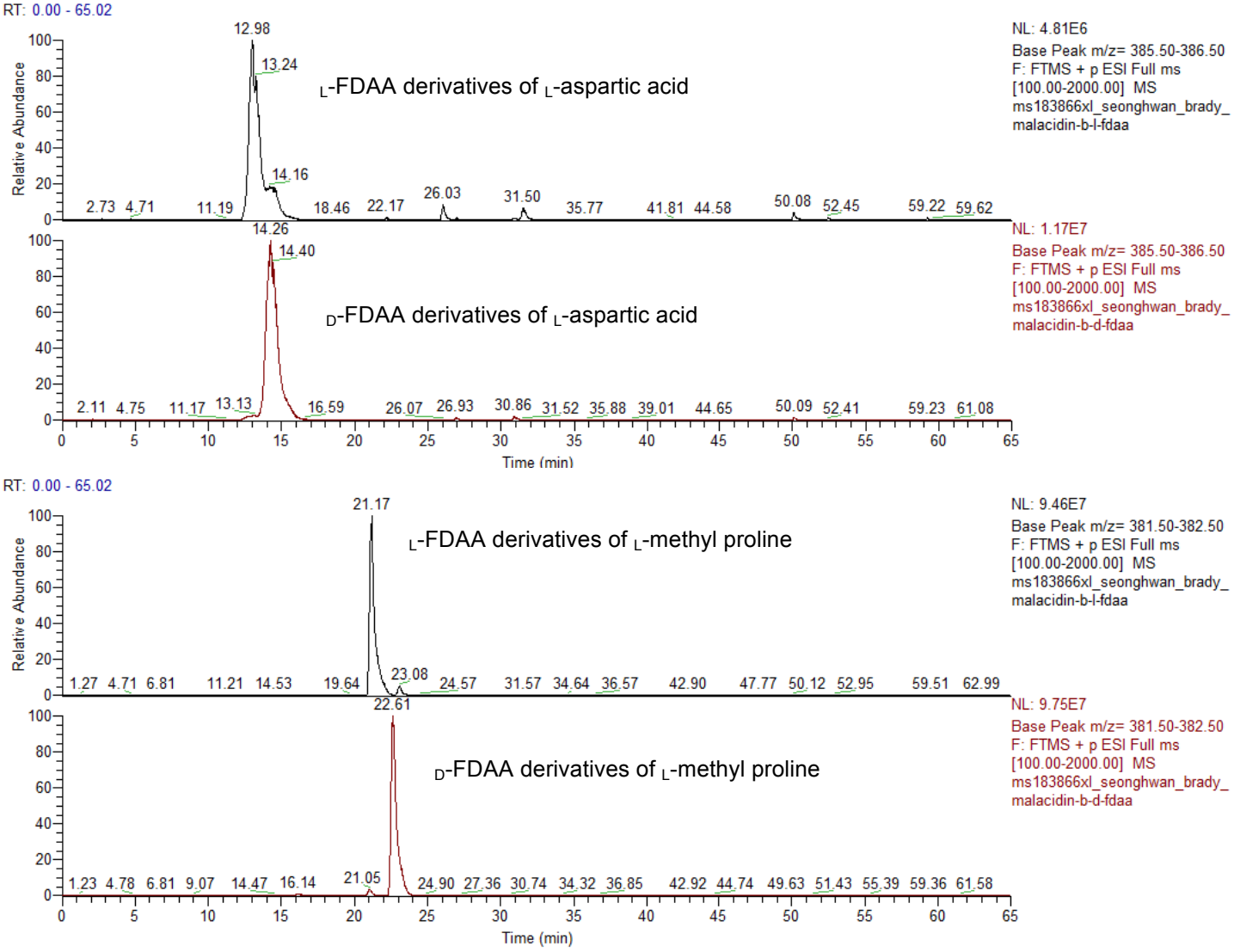
RT: 0.00 - 65.02
Relative Abundance
12.98
13.24
14.16
14.26
$_L$-FDAA derivatives of $_L$-aspartic acid
NL: 4.81E6
Base Peak m/z= 385.50-386.50
F: FTMS + p ESI Full ms
[100.00-2000.00] MS
ms183866xl_seonghwan_brady_
malacidin-b-l-fdaa
14.40
$_D$-FDAA derivatives of $_L$-aspartic acid
NL: 1.17E7
Base Peak m/z= 385.50-386.50
F: FTMS + p ESI Full ms
[100.00-2000.00] MS
ms183866xl_seonghwan_brady_
malacidin-b-d-fdaa
Time (min)

RT: 0.00 - 65.02
Relative Abundance
21.17
$_L$-FDAA derivatives of $_L$-methyl proline
NL: 9.46E7
Base Peak m/z= 381.50-382.50
F: FTMS + p ESI Full ms
[100.00-2000.00] MS
ms183866xl_seonghwan_brady_
malacidin-b-l-fdaa
22.61
$_D$-FDAA derivatives of $_L$-methyl proline
NL: 9.75E7
Base Peak m/z= 381.50-382.50
F: FTMS + p ESI Full ms
[100.00-2000.00] MS
ms183866xl_seonghwan_brady_
malacidin-b-d-fdaa
Time (min)

Figure S23. Proposed biosynthesis of malacidin A.

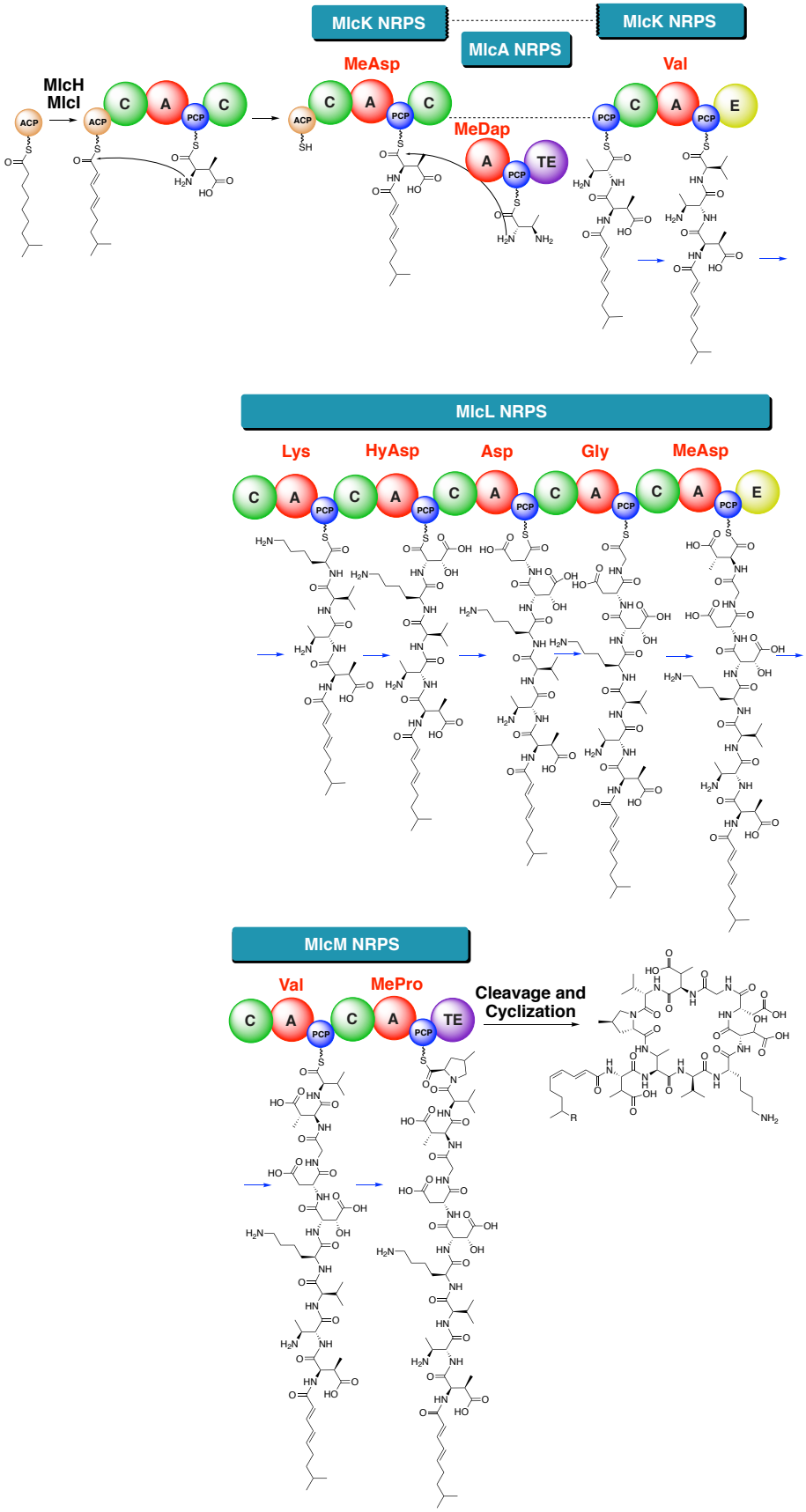

Figure S24. Structural comparison of malacidin to other calcium-dependent antibiotics. **(a)** Malacidin A and B and their general motif compared to **(b)** other previously characterized calcium-dependent antibiotics and **(c)** other Lipid II-binding antibiotics.[12, 13]

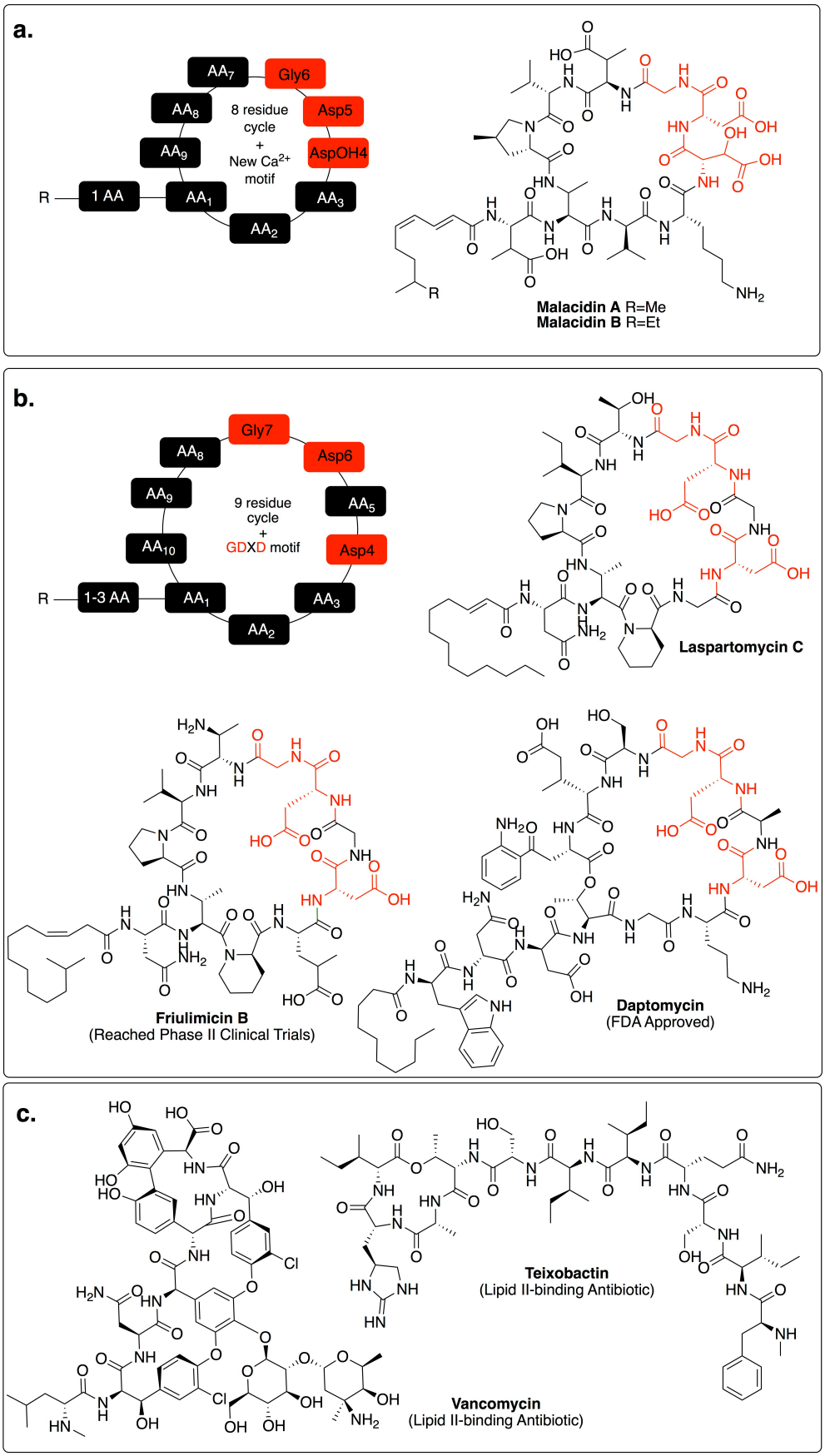

Figure S25. Comparison of malacidin BGC to other calcium-dependent antibiotic gene clusters. (a) Malacidin biosynthetic gene cluster compared to the gene clusters of other representative calcium-dependent antibiotics. The NRPS genes are indicated in light blue with the domain architecture and incorporated amino acids listed below. The rest of the genes are indicated by color: regulatory (green), transport (yellow), amino acid biosynthesis (purple), and fatty acid biosynthesis (red). **(b)** Table of malacidin proteins and their homologs in other representative calcium-dependent antibiotics biosynthetic clusters. Percent identities of these proteins to malacidin are indicated in parenthesis.

a.

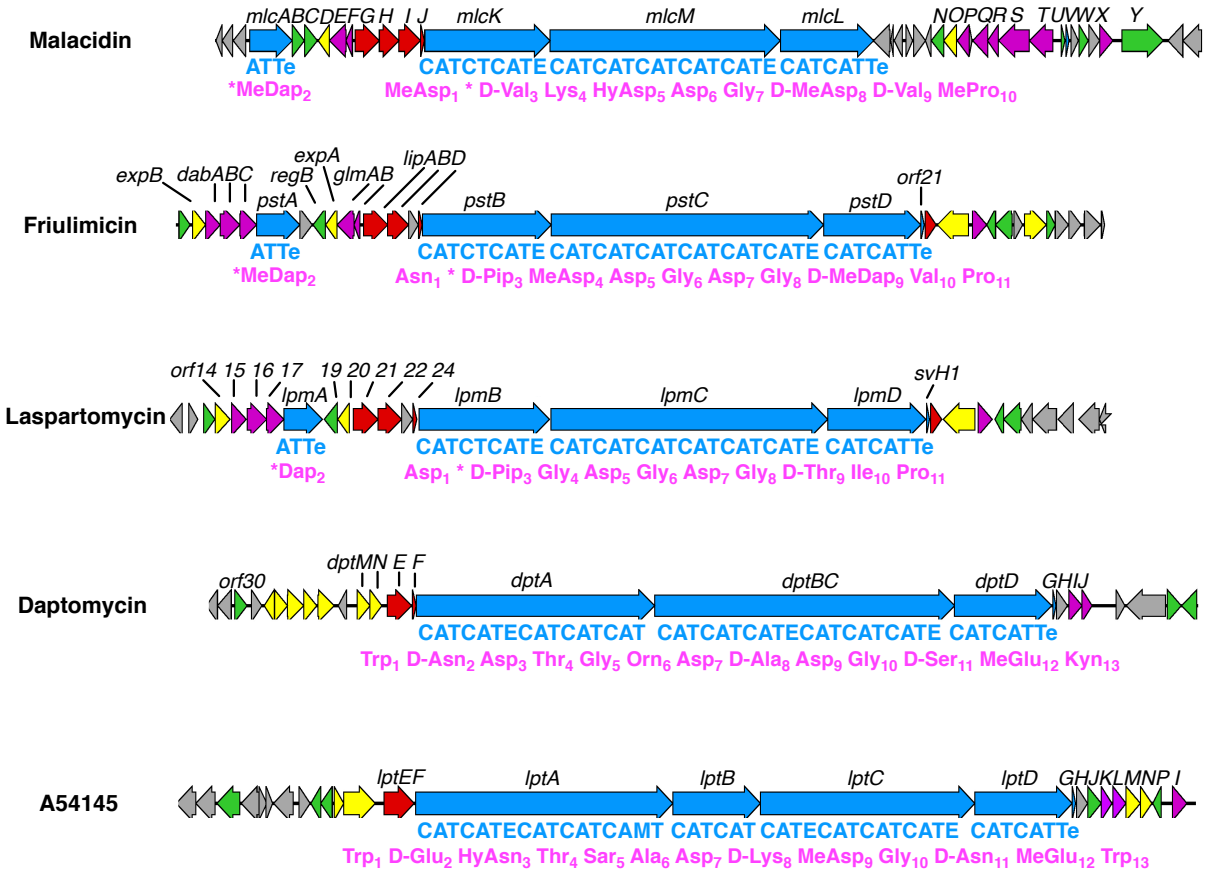

b.

Malacidin	Friulimicin (*A. friuliensis*)	Laspartomycin (*S. viridochromogenes*)	Daptomycin (*S. roseosporus*)	A54145 (*S. fradiae*)
MlcA	PstA (54%)	LpmA (54%)		
MlcB	Orf7 (65%)		Orf30 (65%)	
MlcC				LptJ (62%)
MlcD	ExpA (49%)	Orf20 (47%)	DptN (56%)	LptN (51%)
MlcE	GlmB (59%)			
MlcF	GlmA (60%)			
MlcG	LipA (52%)	Orf21 (54%)	DptE (48%)	LptEF (48%)
MlcH	LipB (52%)	Orf22 (51%)		
MlcI	LipB (24%)	Orf22 (31%)		
MlcJ	LipD (47%)	Orf24 (47%)	DptF (41%)	
MlcK	PstB (50%)	LpmB (50%)	DptA (44%)	LptA (46%)
MlcL	PstC (52%)	LpmC (52%)	DptBC (48%)	LptC (49%)
MlcM	PstD (51%)	LpmD (51%)	DptD (47%)	LptD (46%)
MlcN	RegB (55%)	Orf19 (61%)		LptJ (30%)
MlcO	ExpB (57%)	Orf14 (59%)	DptM (%)	LptM (54%)
MlcP				
MlcQ				
MlcR				
MlcS	DabCA (39%)	Orf15,17 (40%)		
MlcT	DabB (35%)	Orf16 (31%)		
MlcU				
MlcV	Orf21 (71%)	SvH1 (70%)	DptG (68%)	LptG (72%)
MlcW				
MlcX				
MlcY				

Figure S26. Effects of mono- and divalent cations on malacidin activity. Results of serial dilution MIC assays against *S. aureus* USA300 using media supplemented with 15 mM of various mono- and divalent cations. 0.1 mg/mL was the highest concentration tested. Error bars represent the standard error across three replicate experiments.

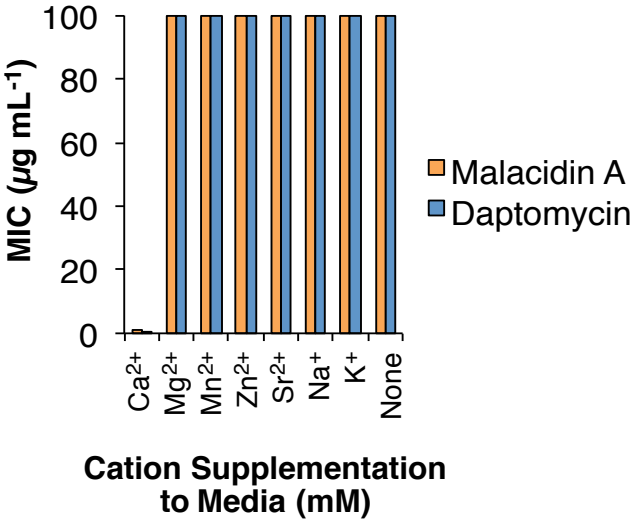

Figure S27. Assessing malacidin A mammalian toxicity. a) Viability assay of two mammalian cell lines, HEK293 (epithelial morphology) and MRC5 (fibroblast morphology), when treated with vehicle or 0.1 mg/mL Malacidin A (100x MIC). Error bars represent the standard error across three biological replicates. b) Malacidin A showed no hemolytic effects over 24 hours when assayed in red blood cell disc diffusion assays. Triton X-100 was used a positive control for lysis. Image of red blood cell plate is representative of three replicate experiments.

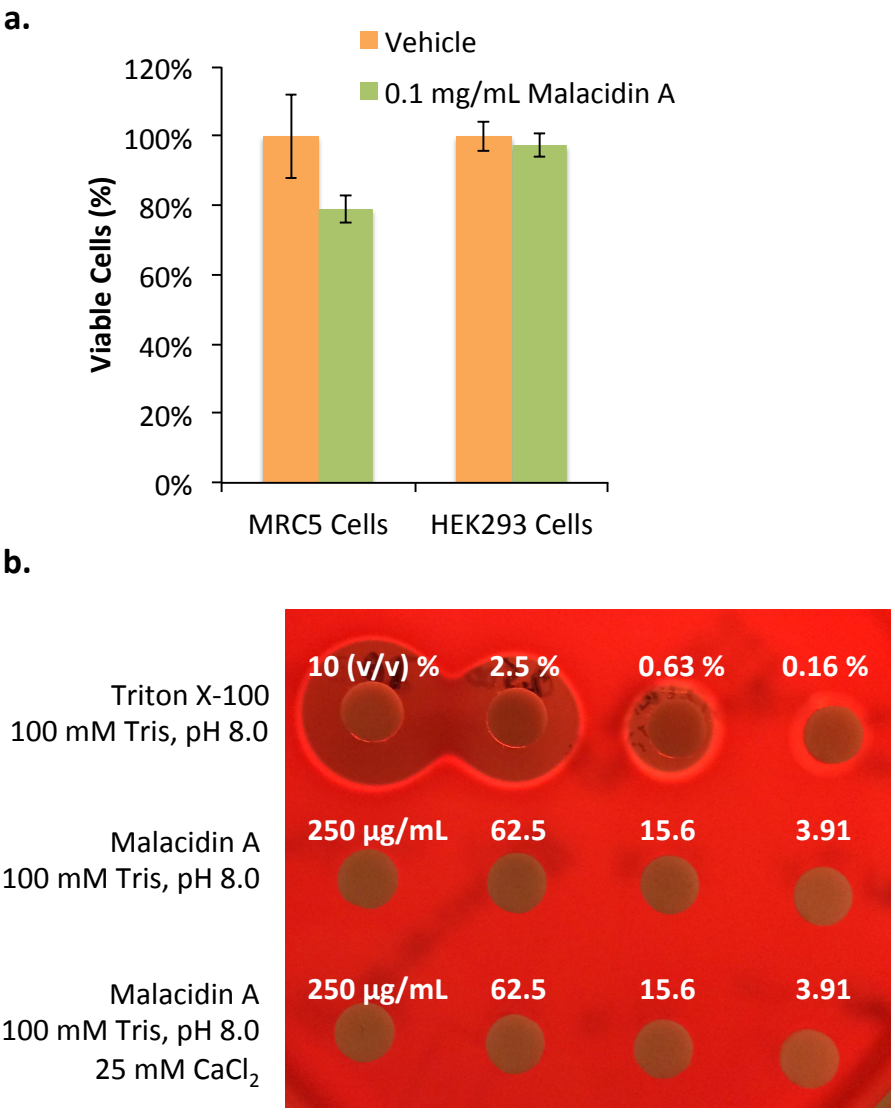

Figure S28. Malacidin does not induce membrane depolarization. In a similar experiment to the SYTOX membrane leakage experiments, the effects of malacidin on membrane depolarization were assessed using the membrane potential probe, $DiBAC_4$ (Bis-(1,3-Dibutylbarbituric Acid)Trimethine Oxonol). Malacidin, in contrast to daptomycin, demonstrated no significant loss of membrane potential when testing against *S. aureus* cells pretreated with $DiBAC_4$. These data along with the SYTOX green assays suggest that malacidin does not cause either significant membrane disruption or leakage of ions. Error bars represent the standard error across three biological replicates.

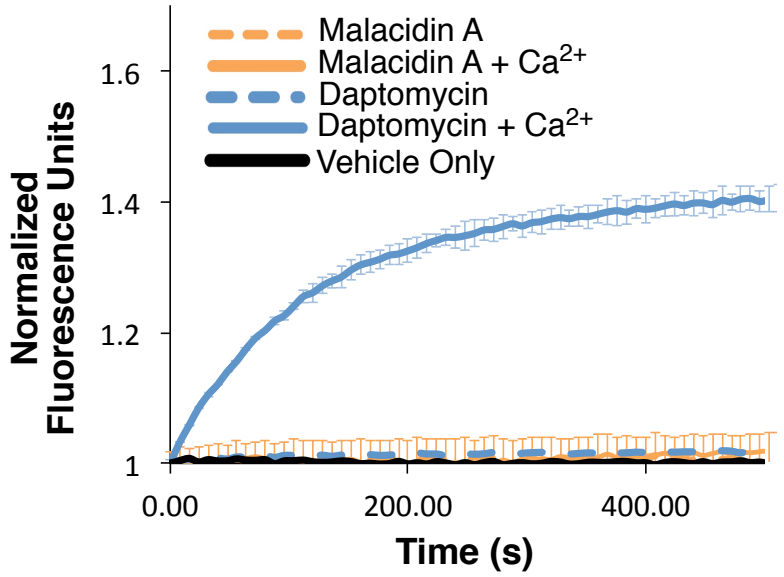

Figure S29. Raw data for thin-layer chromatography. Figures **(a)** 4d and **(b)** 4e in the main text were generated by visualizing on thin-layer chromatography by UV light the amount of free antibiotic after extraction. Images were cropped, desaturated, and the contrast was inverted to maximize visualization.

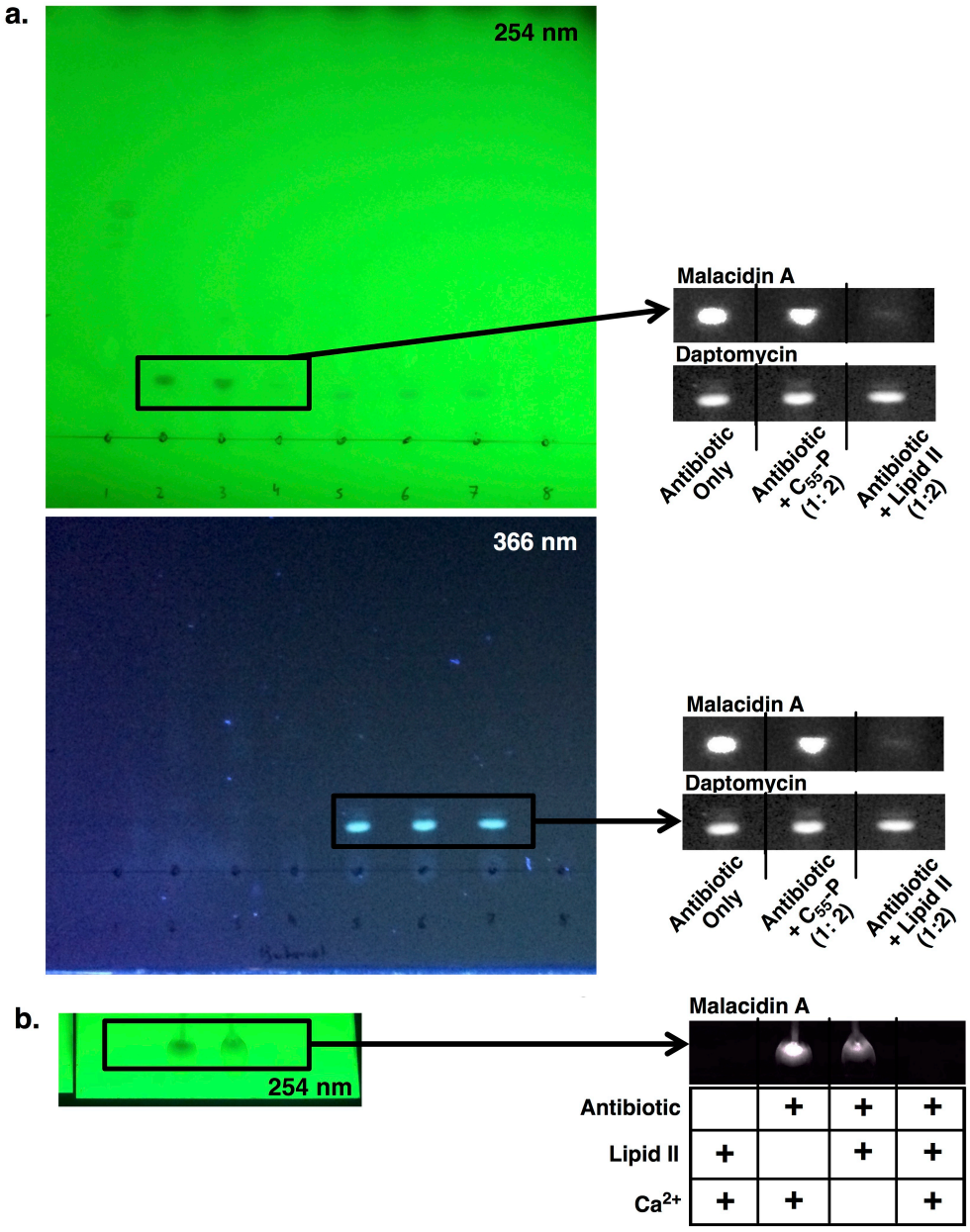

Supplementary References

1. Heinzelmann, E. et al. A glutamate mutase is involved in the biosynthesis of the lipopeptide antibiotic friulimicin in Actinoplanes friuliensis. *Antimicrobial agents and chemotherapy* **47**, 447-457 (2003).
2. Liu, L. et al. 4-Methylproline guided natural product discovery: co-occurrence of 4-hydroxy- and 4-methylprolines in nostoweipeptins and nostopeptolides. *ACS chemical biology* **9**, 2646-2655 (2014).
3. Luesch, H. et al. Biosynthesis of 4-methylproline in cyanobacteria: cloning of nosE and nosF genes and biochemical characterization of the encoded dehydrogenase and reductase activities. *The Journal of organic chemistry* **68**, 83-91 (2003).
4. Muller, C. et al. Sequencing and analysis of the biosynthetic gene cluster of the lipopeptide antibiotic Friulimicin in Actinoplanes friuliensis. *Antimicrobial agents and chemotherapy* **51**, 1028-1037 (2007).
5. Strieker, M. & Marahiel, M.A. The structural diversity of acidic lipopeptide antibiotics. *Chembiochem : a European journal of chemical biology* **10**, 607-616 (2009).
6. Schubert, V. et al. Stereochemistry and conformation of skyllamycin, a non-ribosomally synthesized peptide from Streptomyces sp. Acta 2897. *Chemistry* **20**, 4948-4955 (2014).
7. Fujii, K. et al. A Nonempirical Method Using LC/MS for Determination of the Absolute Configuration of Constituent Amino Acids in a Peptide: Elucidation of Limitations of Marfey's Method and of Its Separation Mechanism. *Analytical Chemistry* **69**, 3346-3352 (1997).
8. Miao, V. et al. Daptomycin biosynthesis in Streptomyces roseosporus: cloning and analysis of the gene cluster and revision of peptide stereochemistry. *Microbiology* **151**, 1507-1523 (2005).
9. Miao, V. et al. The lipopeptide antibiotic A54145 biosynthetic gene cluster from Streptomyces fradiae. *Journal of industrial microbiology & biotechnology* **33**, 129-140 (2006).
10. Wang, Y., Chen, Y., Shen, Q. & Yin, X. Molecular cloning and identification of the laspartomycin biosynthetic gene cluster from Streptomyces viridochromogenes. *Gene* **483**, 11-21 (2011).
11. Medema, M.H. et al. antiSMASH: rapid identification, annotation and analysis of secondary metabolite biosynthesis gene clusters in bacterial and fungal genome sequences. *Nucleic acids research* **39**, W339-346 (2011).
12. Griffith, R.S. Introduction to vancomycin. *Reviews of infectious diseases* **3 suppl**, S200-204 (1981).
13. Ling, L.L. et al. A new antibiotic kills pathogens without detectable resistance. *Nature* **517**, 455-459 (2015).